The Parton Cascade Model and Jet Quenching in Heavy Ion Physics

C.Coleman-Smith
cec24@phy.duke.edu

August 2013

Outline

- The Parton Cascade Model
- Early History: The major VNI results
- A brief and incomplete survey of some other models
- Jets Observables with VNI/BMS Box Mode
- What Next?

The Parton Cascade Model

- Describes the time evolution of a system of quarks and gluons, a microscopic transport model based upon the Boltzmann equation.

$$p^\mu \frac{\partial}{\partial x^\mu} F_k(x,p) = \sum \mathcal{C}_i F(x,p)$$

- Particles follow classical trajectories in phase space. Full relativistic mechanics for scattering kinematics

- A geometric interpretation of the cross-section is used to select interactions

- Collision term is potentially very general. Usually models consider 2->2 processes (binary scatterings) and radiative processes 1->2, 2->N.

- Not clear how to propagate virtual particles.

Parton Cascades - Past Historical

VNI - K.Geiger & B.Müller (1991)

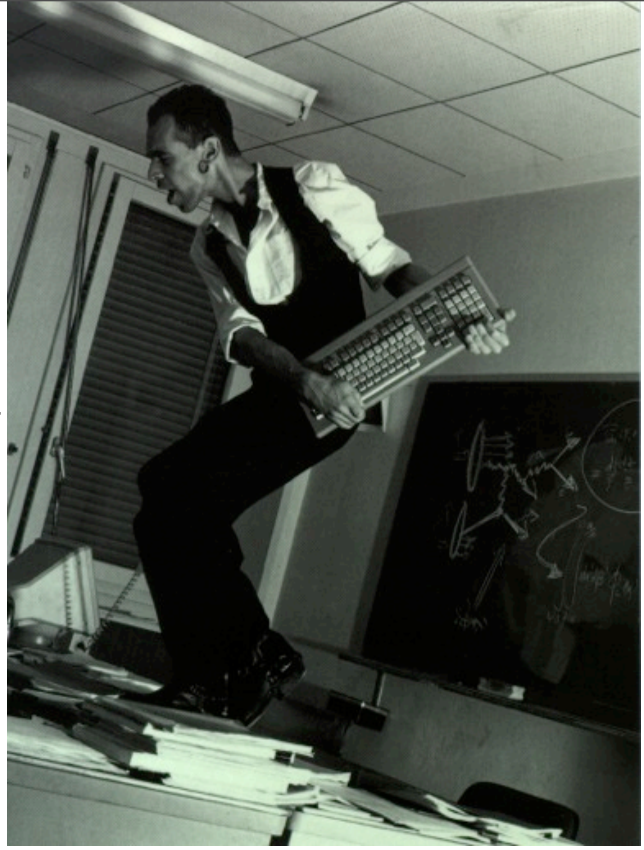

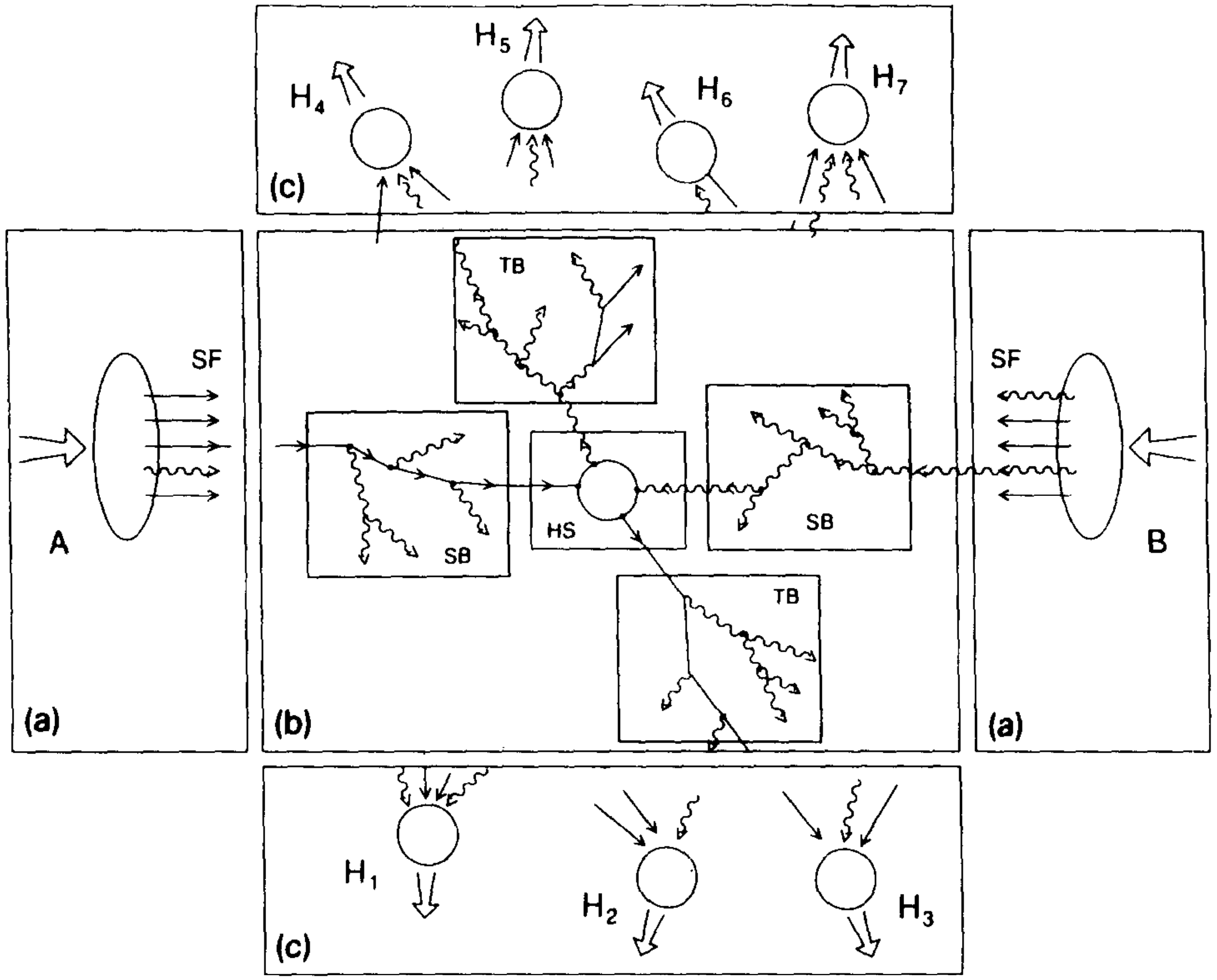

- Full set of 2->2 scatterings
- Space-like and time-like branching processes.
- Some off-shell propagation is mooted, not totally clear how it worked in practice
- Global pt cut-off for hard scatterings.
- Partons sampled from PDF's with slightly fuzzy spatial distributions
- Predictions of multiplicity and energy deposition in central region

Parton Cascade Model, designed to describe the energy deposition, thermalization and chemical equilibration of matter in high-energy nuclear collisions

K.Geiger & B.Müller. N Phys B **369** (1992)

Thermalization - VNI

Thermalization in ultrarelativistic nuclear collisions.
I. Parton kinetics and quark-gluon plasma formation

Klaus Geiger
School of Physics and Astronomy, University of Minnesota, Minneapolis, Minnesota 55455
(Received 10 March 1992)

- Added a lot of soft & phenomenological effects
- Simple LPM Effect
- Smearing soft parton distributions
- Competitive Emission and absorbtion
- Soft Cross-Section

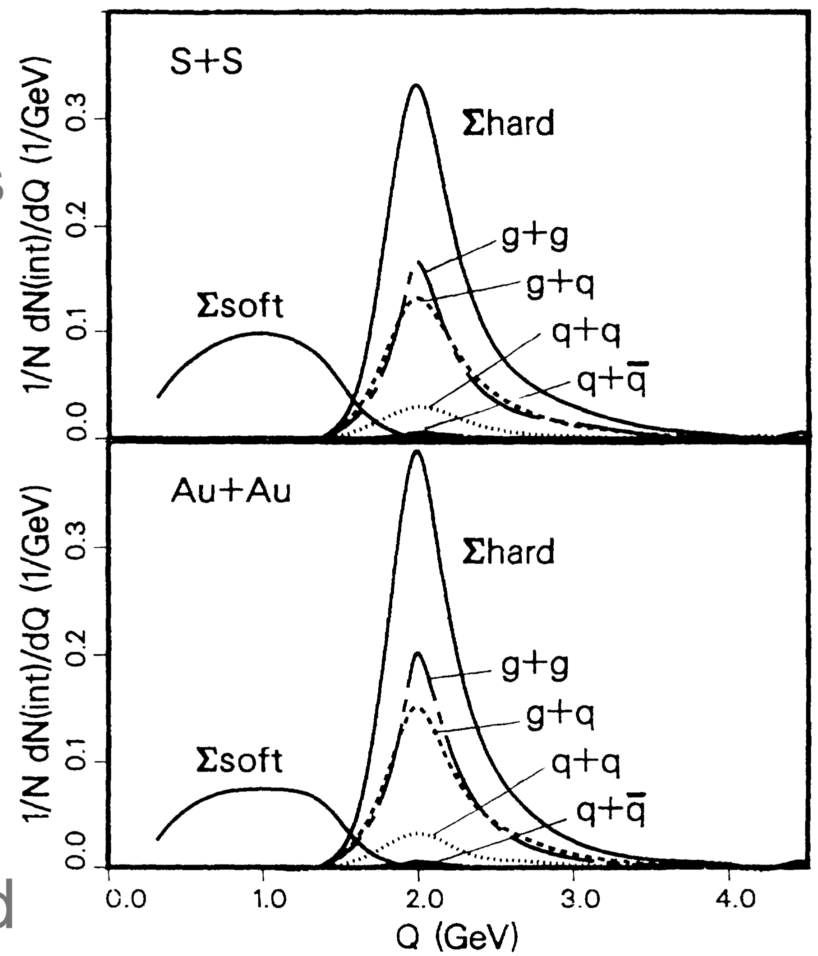

FIG. 5. Relative contributions of (semi)hard and soft parton-parton collisions in ^{32}S+^{32}S and ^{197}Au+^{197}Au ($\sqrt{s}=200A$ GeV). Shown are the differential probabilities $dP_{\rm int}/dQ$ as a function of $Q=p_\perp$ (full lines). The (semi)hard collisions are in addition split up into the individual contributions from $g+g$, $g+q$, $q+q$, and $q+\bar{q}$.

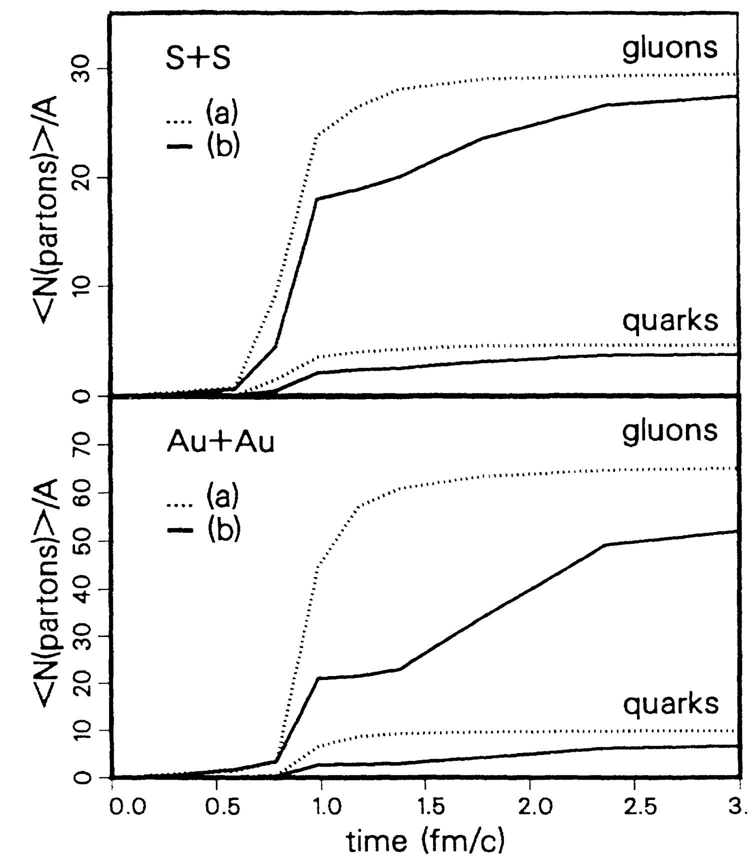

FIG. 3. Average cumulative number of secondary gluons and quarks per nucleon produced during collisions of ^{32}S+^{32}S and ^{197}Au+^{197}Au at $\sqrt{s}=200A$ GeV. The plots (a) and (b) refer to the two space-time evolution scenarios explained in the text.

K.Geiger, Phys Rev D **46**, (4965) (1992),
K.Geiger, Phys Rev D **46**, (4986) (1992)

Thermalization - VNI

Thermalization in ultrarelativistic nuclear collisions.
I. Parton kinetics and quark-gluon plasma formation

Klaus Geiger
School of Physics and Astronomy, University of Minnesota, Minneapolis, Minnesota 55455
(Received 10 March 1992)

- Added a lot of soft & phenomenological effects
- Simple LPM Effect
- Smearing soft parton distributions
- Competitive Emission and absorbtion
- Soft Cross-Section

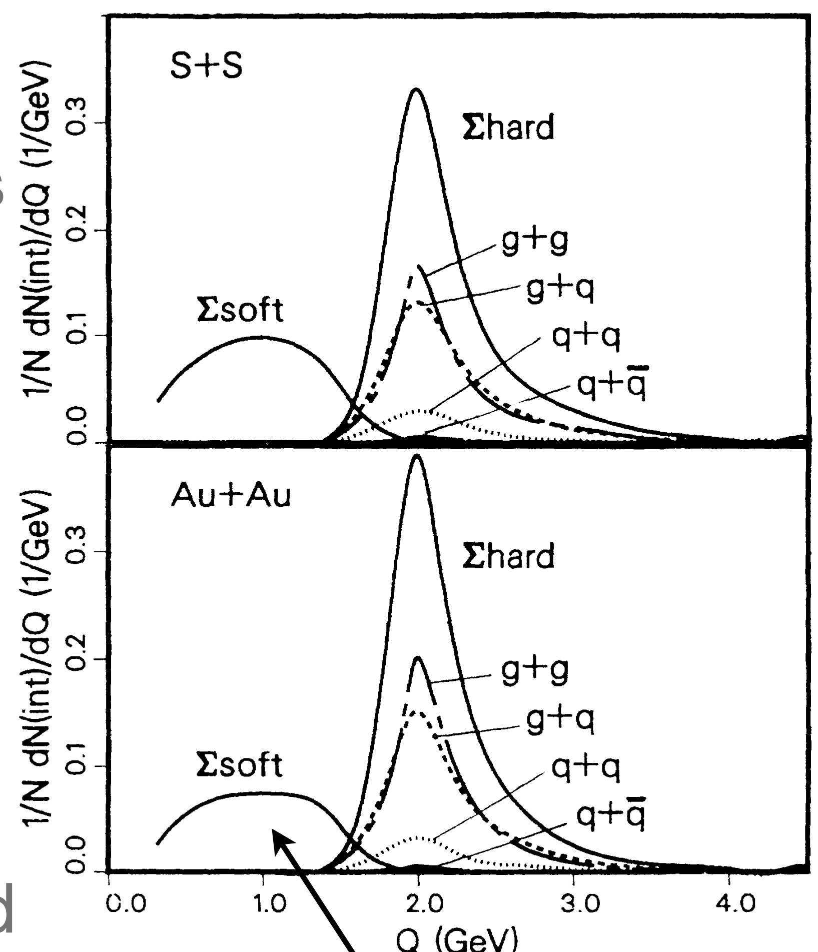

FIG. 5. Relative contributions of (semi)hard and soft parton-parton collisions in $^{32}S+^{32}S$ and $^{197}Au+^{197}Au$ ($\sqrt{s} = 200A$ GeV). Shown are the differential probabilities $dP_{\rm int}/dQ$ as a function of $Q = p_\perp$ (full lines). The (semi)hard collisions are in addition split up into the individual contributions from $g+g$, $g+q$, $q+q$, and $q+\bar{q}$.

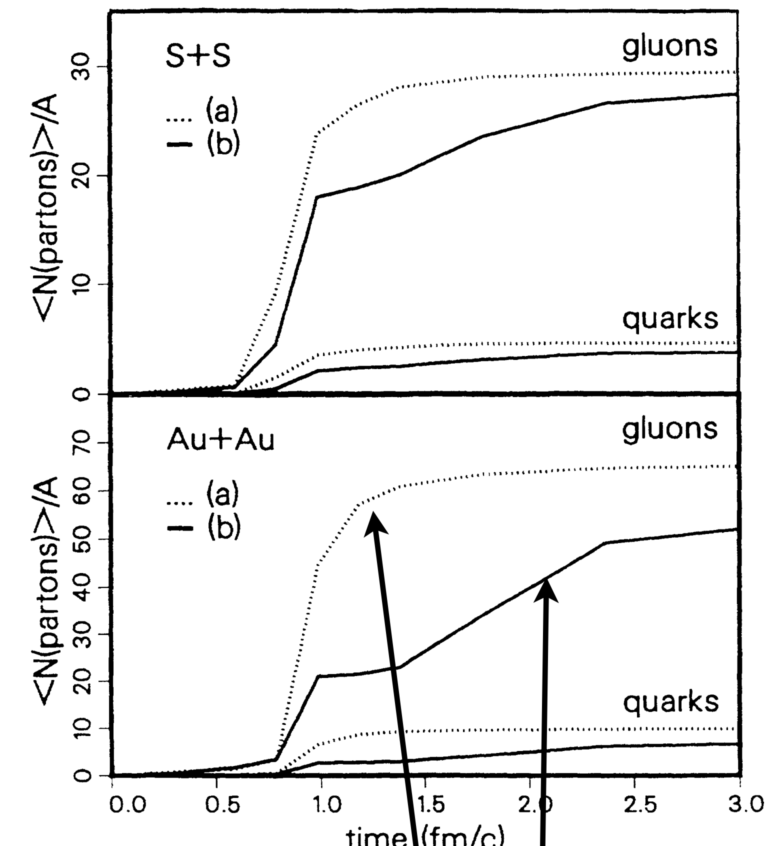

FIG. 3. Average cumulative number of secondary gluons and quarks per nucleon produced during collisions of $^{32}S+^{32}S$ and $^{197}Au+^{197}Au$ at $\sqrt{s} = 200A$ GeV. The plots (a) and (b) refer to the two space-time evolution scenarios explained in the text.

phenomenological soft cross-section

Multiplicity is dominated by radiated gluons

K.Geiger, Phys Rev D **46**, (4965) (1992),
K.Geiger, Phys Rev D **46**, (4986) (1992)

Thermalization - VNI

Thermalization in ultrarelativistic nuclear collisions.
II. Entropy production and energy densities at
the BNL Relativistic Heavy Ion Collider and the CERN Large Hadron Collider

Klaus Geiger
School of Physics and Astronomy, University of Minnesota, Minneapolis, Minnesota 55455
(Received 5 May 1992)

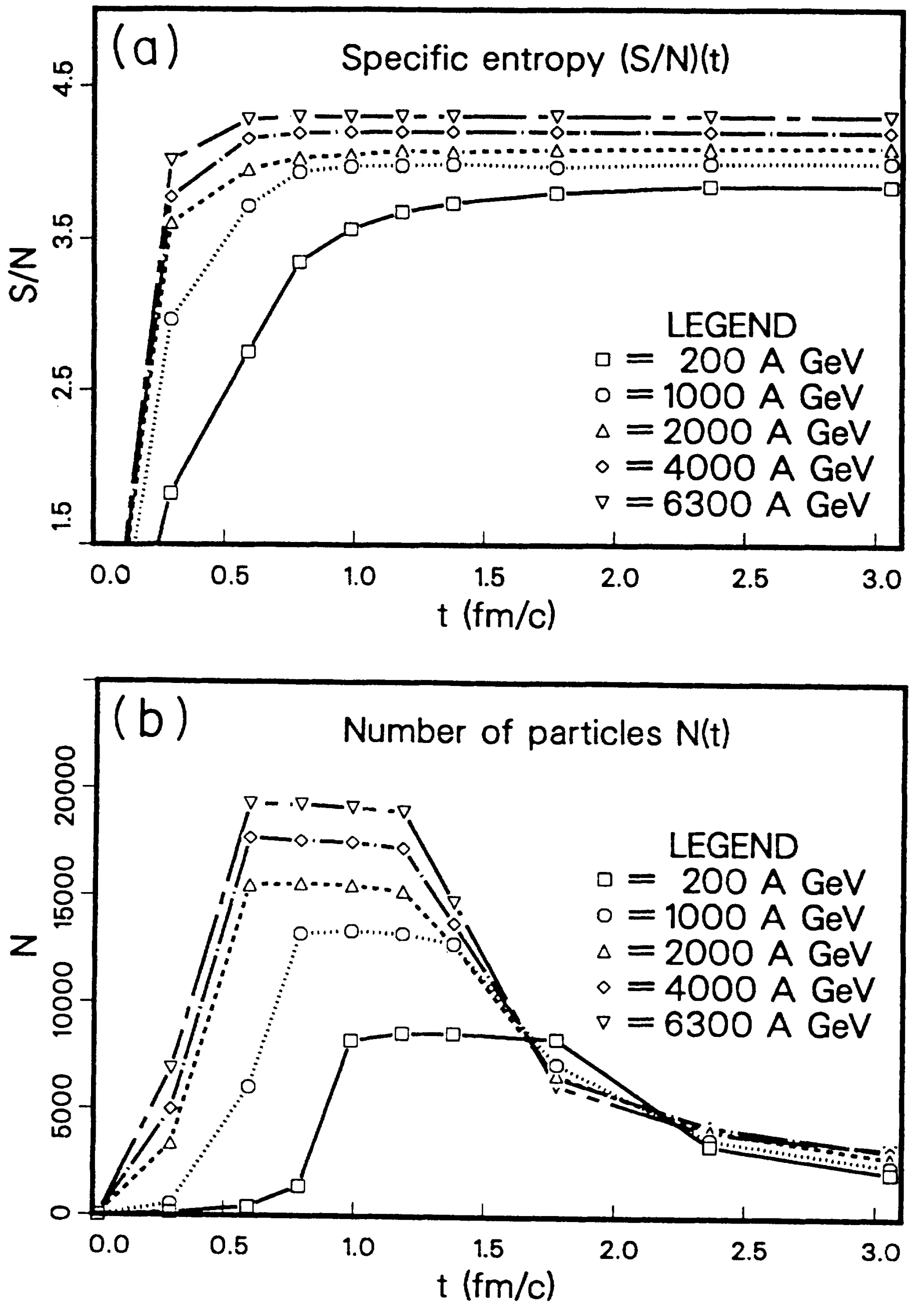

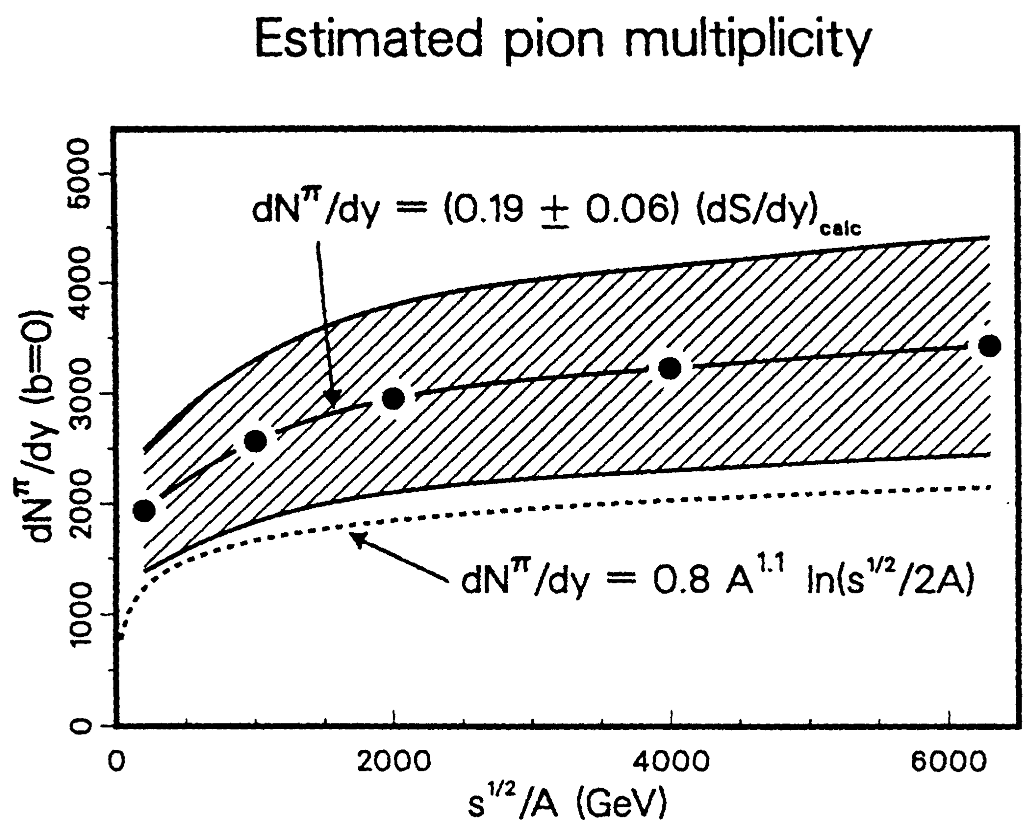

FIG. 14. The pion multiplicities in the central rapidity region around $y = 0$ estimated from the amount of total entropy in the central unit of rapidity, dS/dy, produced by the secondary partons during Au + Au collisions with $\sqrt{s} = 200A$–$6300A$ GeV. The points result from the computed values of dS/dy for the beam energies $\sqrt{s} = 200A$–$6300A$ GeV. Note that the predictions are based on the estimated ratio $r = 0.7 \pm 0.2$ of entropy densities between pion gas and quark-gluon plasma, which results in relatively large uncertainties as indicated by the shaded strip between the full curves. For comparison, the dotted curve corresponds to a more moderate empirical estimate for the multiplicity of pions obtained by extrapolation from pp and pA data.

K.Geiger, Phys Rev D **46**, (4965) (1992),
K.Geiger, Phys Rev D **46**, (4986) (1992)

Thermalization in ultrarelativistic nuclear collisions. II. Entropy production and energy densities at the BNL Relativistic Heavy Ion Collider and the CERN Large Hadron Collider

Klaus Geiger
School of Physics and Astronomy, University of Minnesota, Minneapolis, Minnesota 55455
(Received 5 May 1992)

Thermalization - VNI

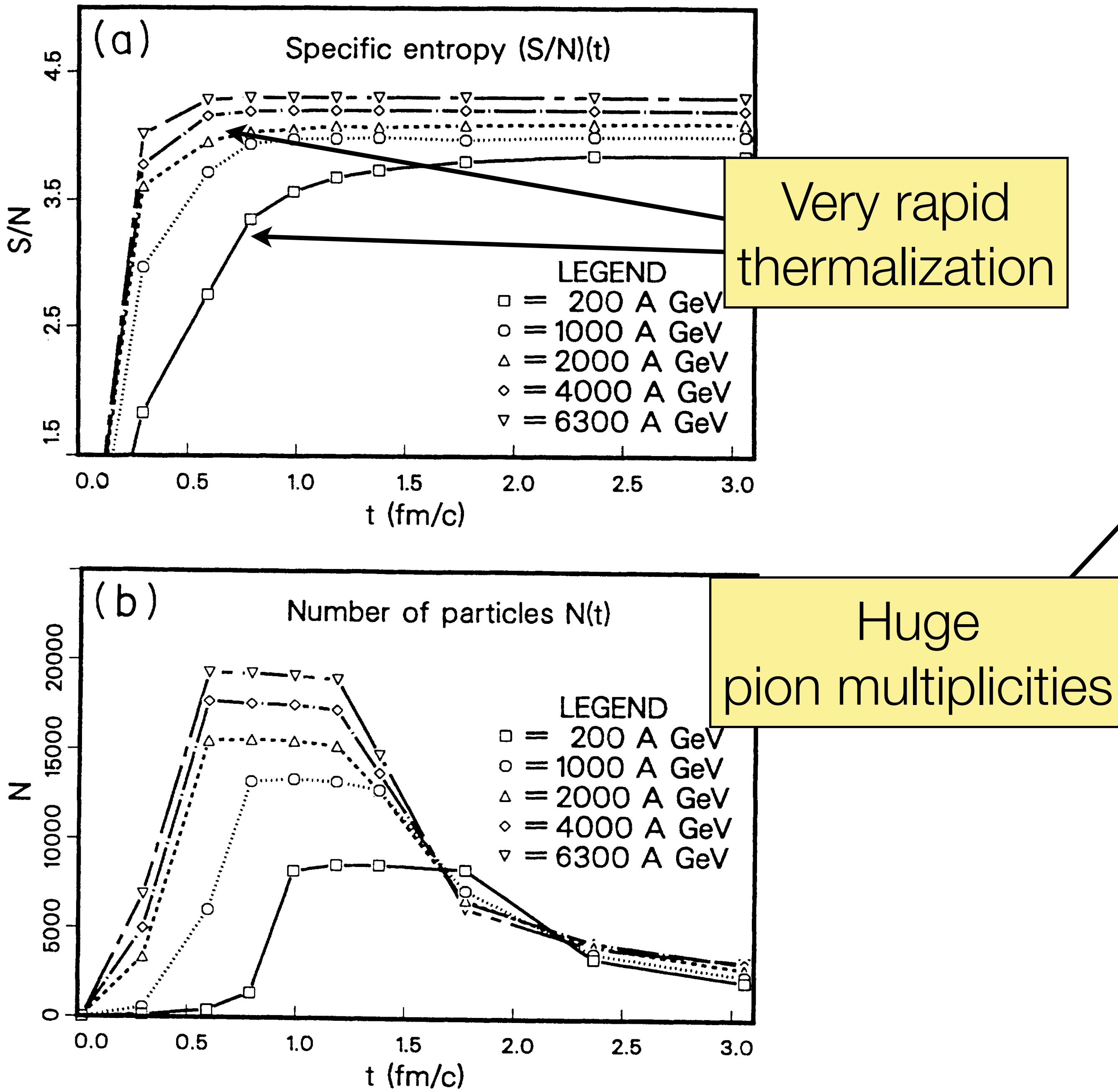

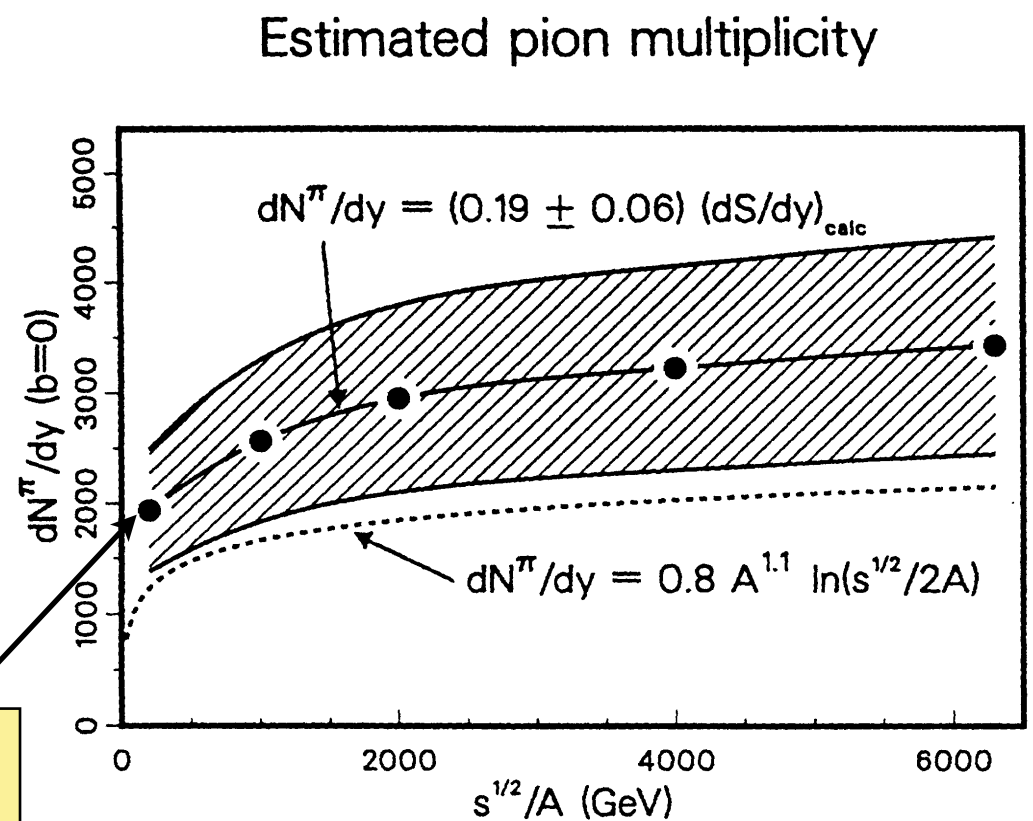

FIG. 14. The pion multiplicities in the central rapidity region around $y = 0$ estimated from the amount of total entropy in the central unit of rapidity, dS/dy, produced by the secondary partons during Au + Au collisions with $\sqrt{s} = 200A$–$6300A$ GeV. The points result from the computed values of dS/dy for the beam energies $\sqrt{s} = 200A$–$6300A$ GeV. Note that the predictions are based on the estimated ratio $r = 0.7 \pm 0.2$ of entropy densities between pion gas and quark-gluon plasma, which results in relatively large uncertainties as indicated by the shaded strip between the full curves. For comparison, the dotted curve corresponds to a more moderate empirical estimate for the multiplicity of pions obtained by extrapolation from pp and pA data.

K.Geiger, Phys Rev D **46**, (4965) (1992),
K.Geiger, Phys Rev D **46**, (4986) (1992)

VNI/BMS - Bass, Müller & Srivastava (2002)

- Hard Pt cutoff is related to the color screening mass instead of being purely phenomenological

$$\mu_D^2 = -\frac{3\alpha_s}{\pi^2} \lim_{|\vec{q}|\to 0} \int d^3p \, \frac{|\vec{p}|}{\vec{q}\cdot\vec{p}} \vec{q}\cdot\nabla_{\vec{p}} \left[F_g(\vec{p}) + \frac{1}{6}\sum_q \{F_q(\vec{p}) + F_{\bar{q}}(\vec{p})\} \right],$$

- Color screening mass is **not** dynamically calculated, typical values are used to regulate cross-sections

- Removed all the soft processes

- Replaced uniform time-stepping with collision finding routines (more efficient)

- Added photons to the 2->2 and 2->N processes

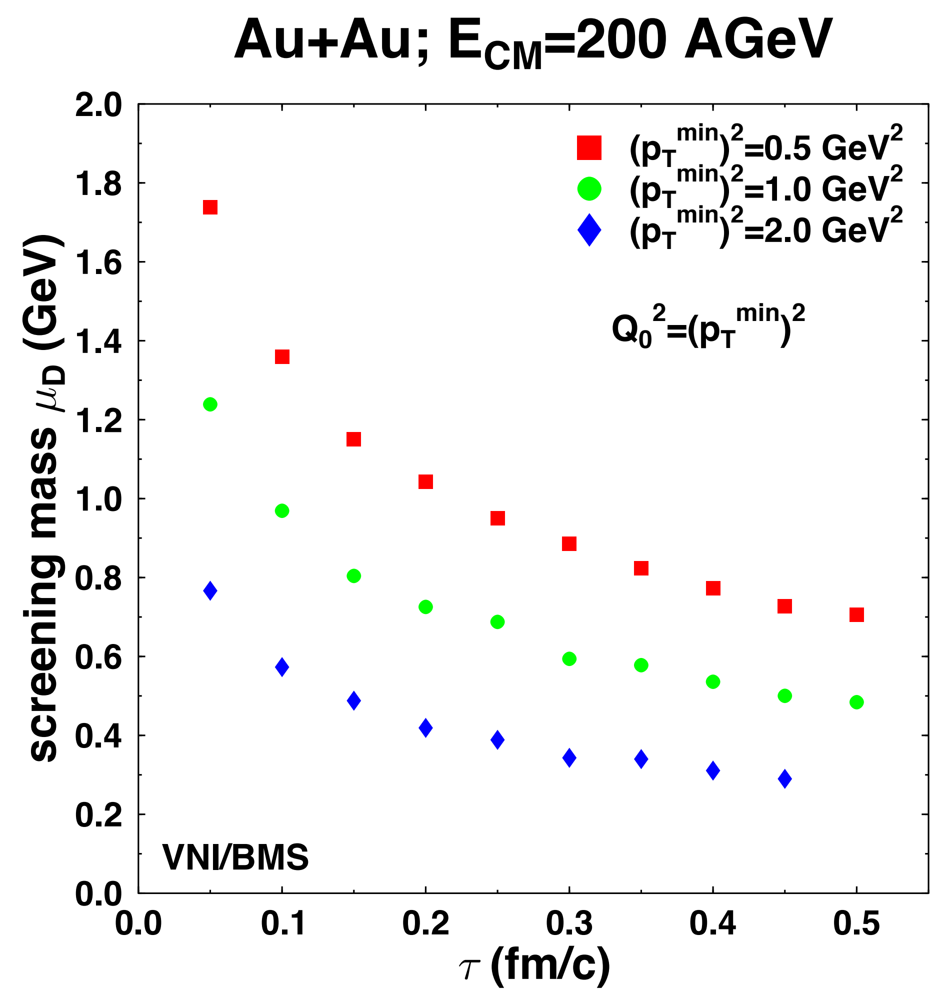

S.A.Bass, B.Müller, D.K.Srivastava. Phys Lett B.**551** (2003)

Stopping at RHIC: VNI/BMS Results

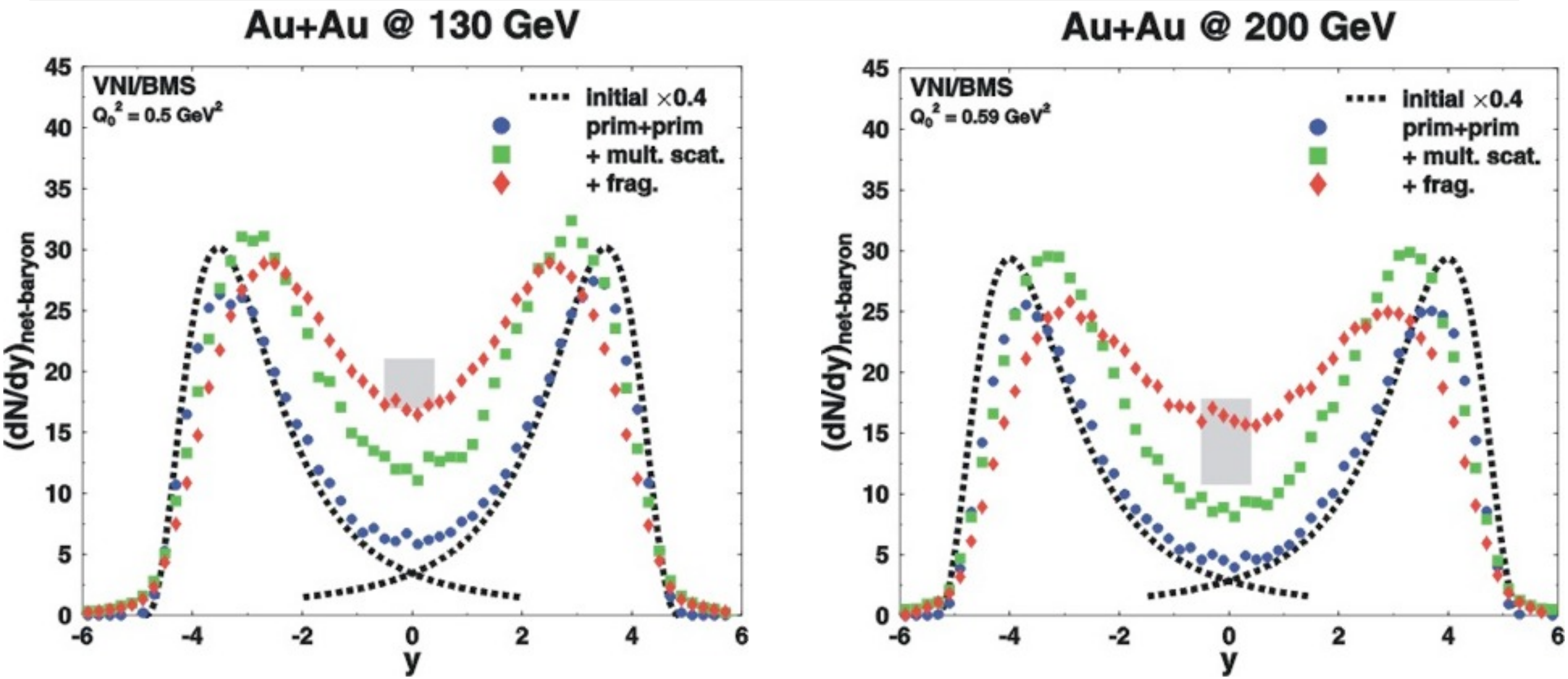

- A lot of effort figuring out a reasonable set of cutoffs for AA
- Multiplicity at mid rapidity works

S.A.Bass, B.Müller, D.K.Srivastava. PRL **91** (2003)

Many Other Models Arose

- ZPC (1999). Gluon only, forms the PCM core of AMPT, Parton Subdivision
- MPC (2000). Subdivision of particles, broad set of included processes
- AMPT (2004). Hybrid transport code, includes stringy effects
- BAMPS (2005). Uses subdivision and a grid, rate based approach naturaly allows for 2->3 and 3->2. Big problems with GB matrix element
- Andong (2002). Full set of 2->2 processes, 2->3 gluon branching, uses a retarded-potential like approach to address causality issues
- These were all relatively successful (or not) at predicting some bulk properties

ZPC: nucl-th/9709009
MPC: nucl-th/0104018
AMPT: nucl-th/9907017, nucl-th/041110
BAMPS: hep-ph/0406278
Andong: nucl-th/0207041

MPC

- Subdivide partons to avoid causality problems inherent in geometric interpretation of the cross-section.
- Fully covariant formulation, uses scaling properties of Boltzmann equation.
- Used very large transport cross-sections to obtain thermal equillbrium
- Under current development, now includes fully covariant support for 1->2 and 2->1 interactions.

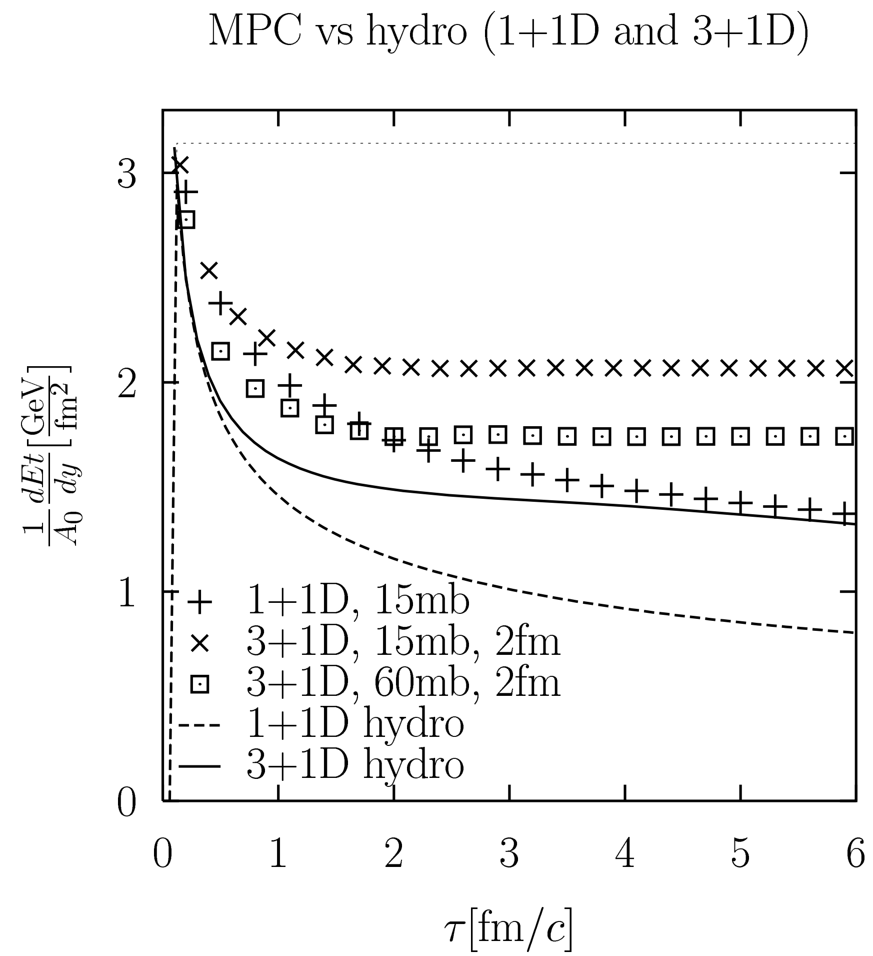

FIG. 1. This figure shows the evolution of the transverse energy dE_t/dy at midrapidity, normalized by the initial transverse area, from kinetic theory and from hydrodynamics both for 1+1 (transverse periodic) and 3+1 dimensions. The initial distribution was a Bjorken cylinder with a radius $R_0 = 2$ fm at proper time $\tau_0 = 0.1$ fm/c in local thermal and chemical equilibrum at $T_0 = 500$ MeV. The cross sections were $\sigma = 15$ and 60 mb, with the cutoff

Molnar & Gyulassy nucl-th/0005051 (2000)

AMPT - A Parton Cascade + ...

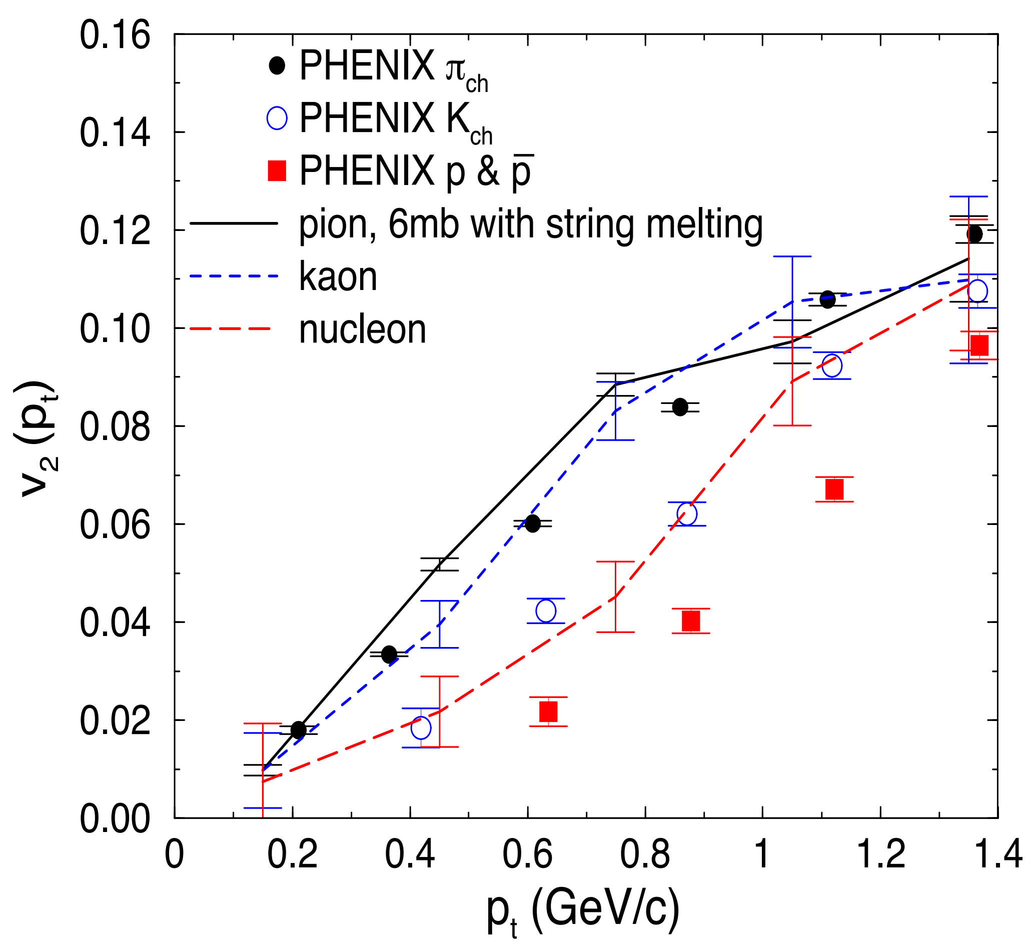

FIG. 29: (Color online) Transverse momentum dependence of elliptic flow of identified hadrons for minimum-bias Au+Au collisions at $\sqrt{s_{NN}} = 200$ GeV. Circles are data from the PHENIX Collaboration [208] while curves are results from the AMPT model with string melting and using 6 mb for the parton scattering cross section.

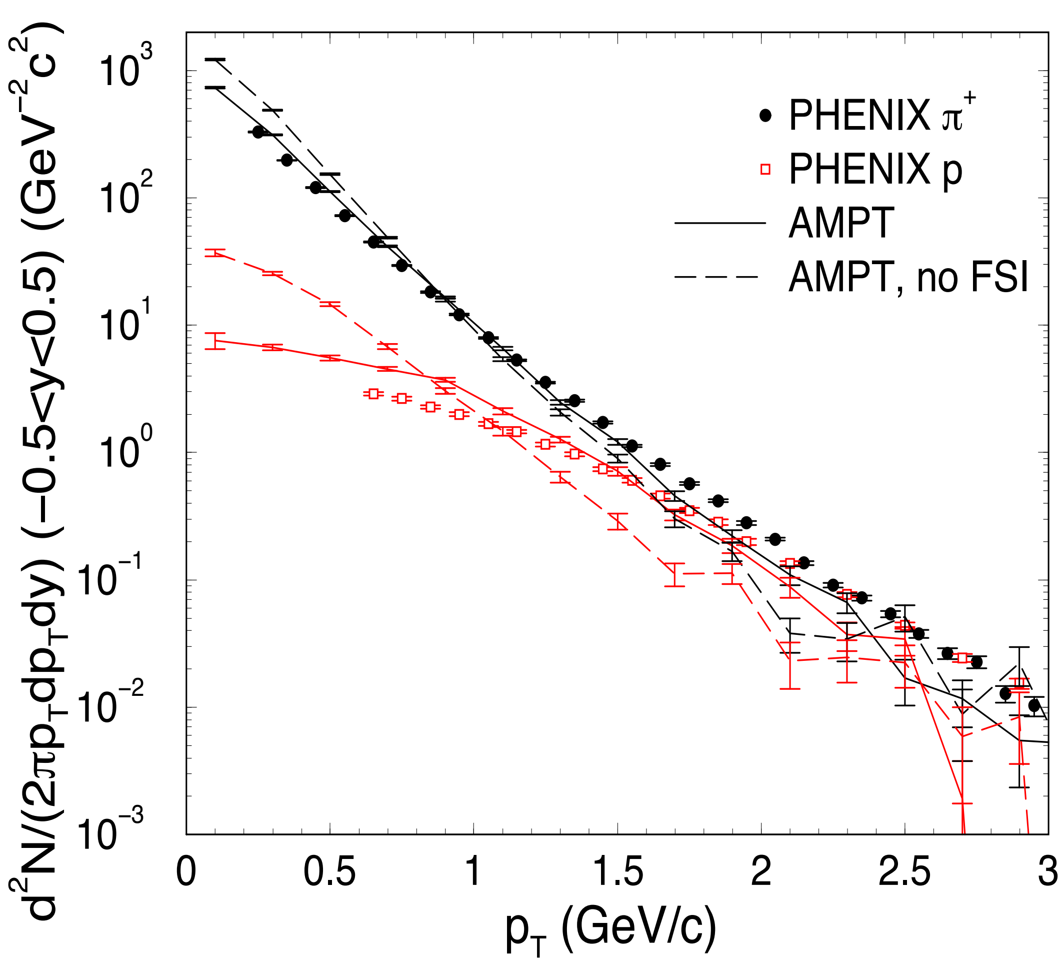

FIG. 25: (Color online) Transverse momentum spectra of mid-rapidity pions and protons from the default AMPT model with (solid curves) and without (dashed curves) final-state interactions in central Au+Au collisions at $\sqrt{s_{NN}} = 200$ GeV.

String melting fits flow

Regular model fits spectra

Parton Cascades - Jet Observables

BAMPS

- a Boltzmann Approach for MultiParticle Scattering
- Uses sub-division partons and a spatial grid, allows for a rate based interpretation of the collision term.
- Rate based approach naturally allows for 2->3 and 3->2 processes
- Dogged by problems in the 2->3 (Gunion-Bertsch) cross-section.
- Problem was finally tracked down in 2013, small rapidity approximations in GB calculation.

BAMPS:
Z. Xu and C. Greiner, PRC 71, 064901 (2005);
Z. Xu and C. Greiner, PRC 76, 024911 (2007)

GB Correction:
Fochler.O et al, hep-ph/1302.5250

BAMPS: Raa and Flow at LHC

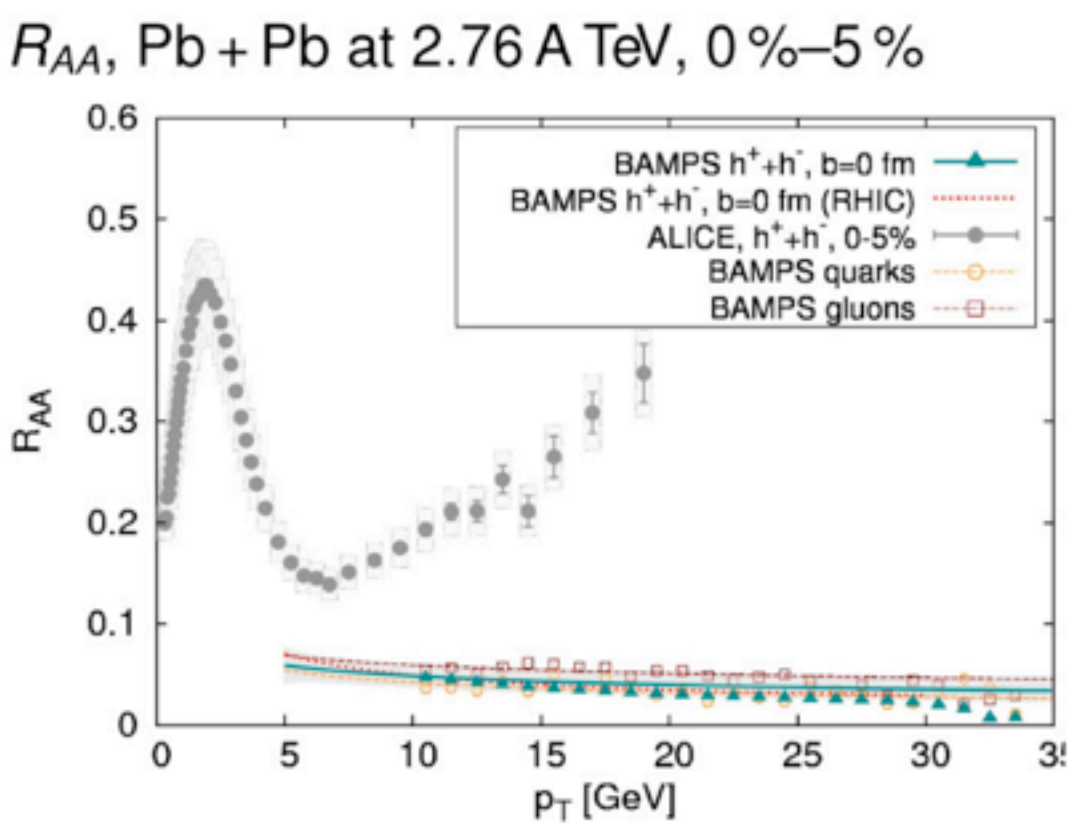

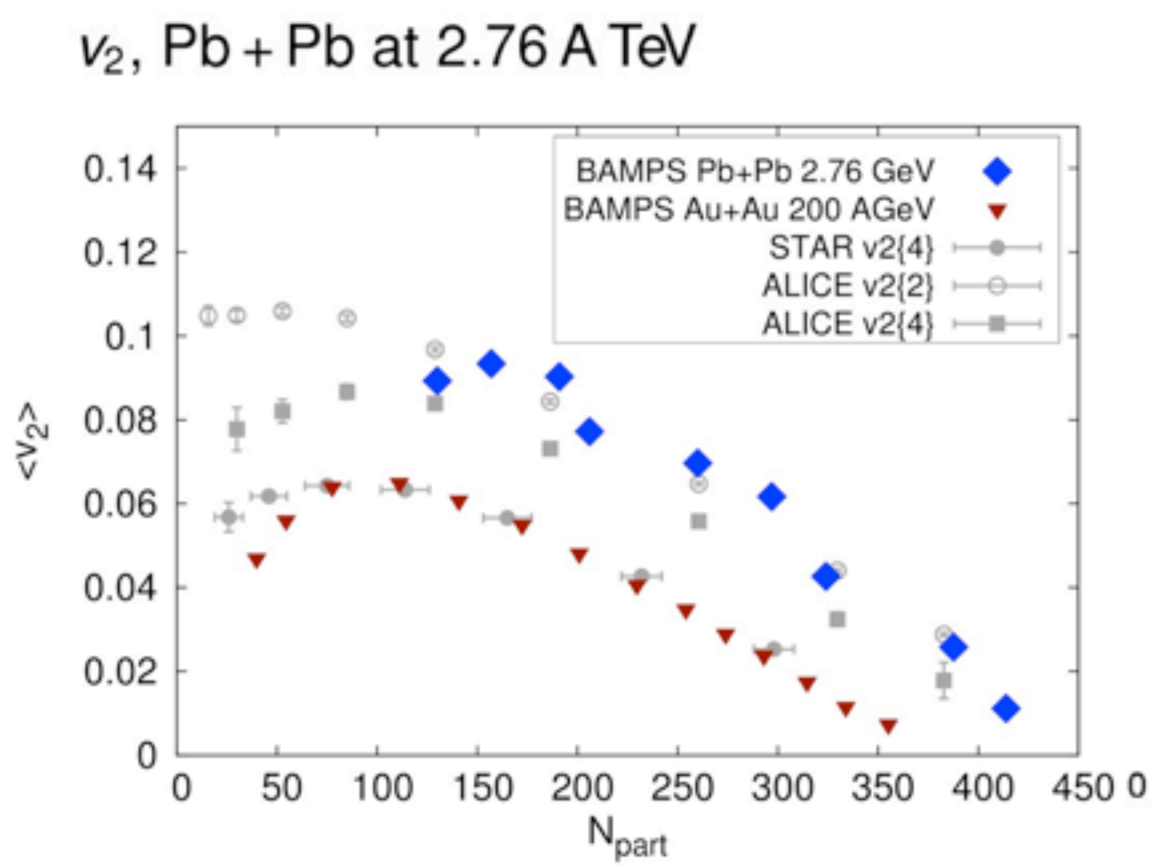

- Pythia Initial Conditions (Uphoff, Fochler et al, PRC 82 (2010)) $\alpha_s = 0.3$
- Raa similar to RHIC, doesn't rise at high Pt.
- Integrated V2 shows increase, drops below data at about 50% centrality

O. Fochler et al, J. Phys. G 38 (2011)

BAMPS: Heavy Quark V2 and Raa at RHIC

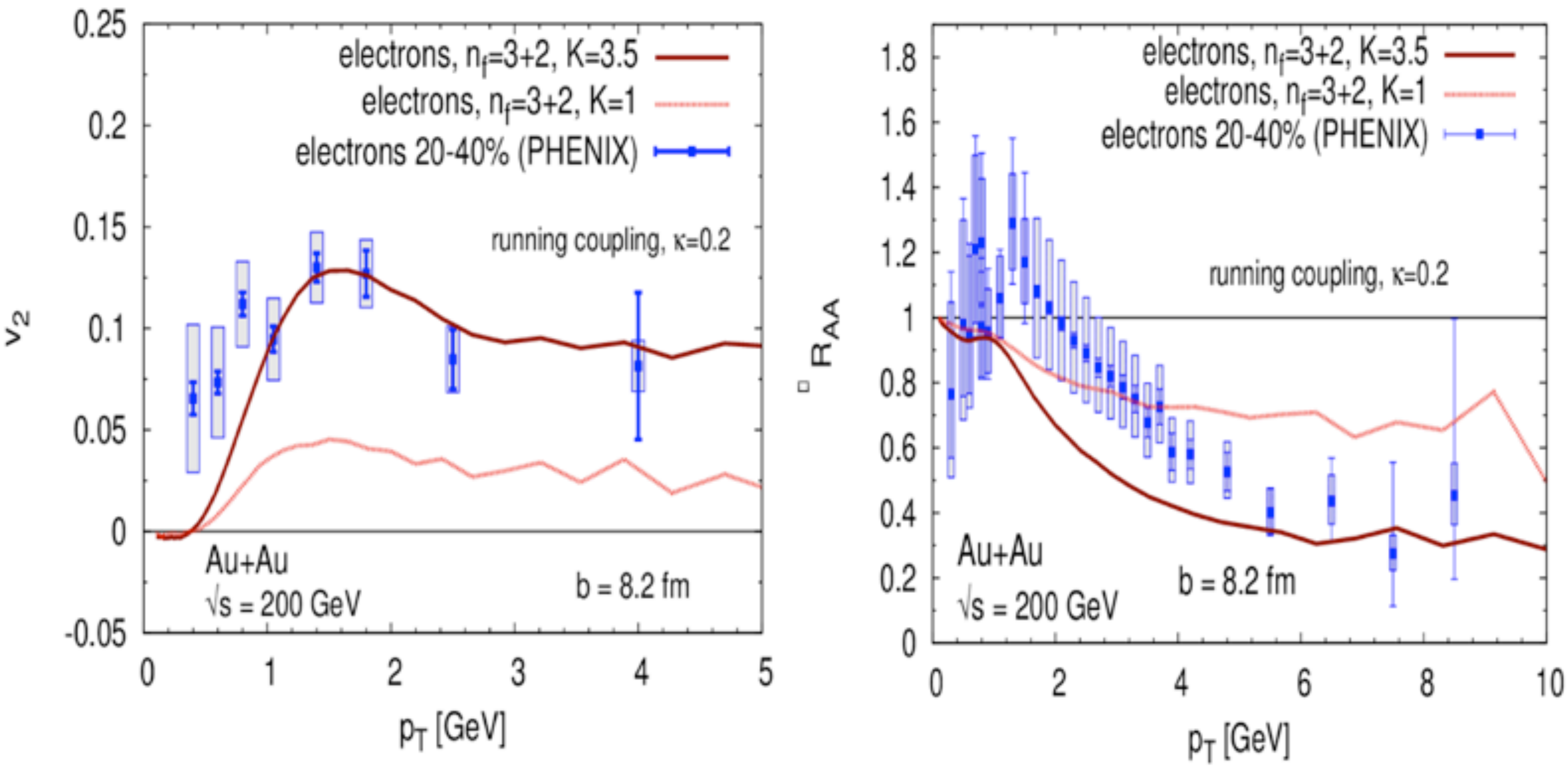

- Needs a large K factor (cross section scaling) to approach data
- Petersen Fragmentation Model: independent fragmentation

Uphoff, Fochler, Xu, CG Phys. Rev. C84 (2011)

BAMPS: Mach Cones ...

Setup

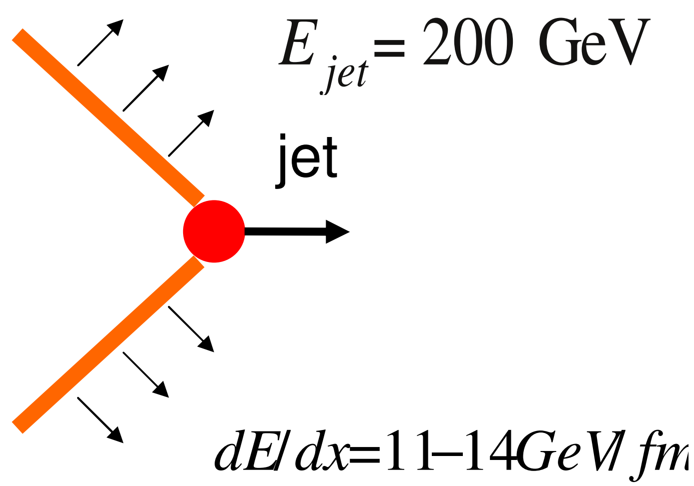

Jet has constant mean free path and only momentum in z-direction!

Medium $T = 400$ MeV

Box scenario, no expansion of the medium, massless Boltzmann gas interactions: 2 –> 2 with isotropic distribution of the collision angle

Looks nice, not a very realistic calculation

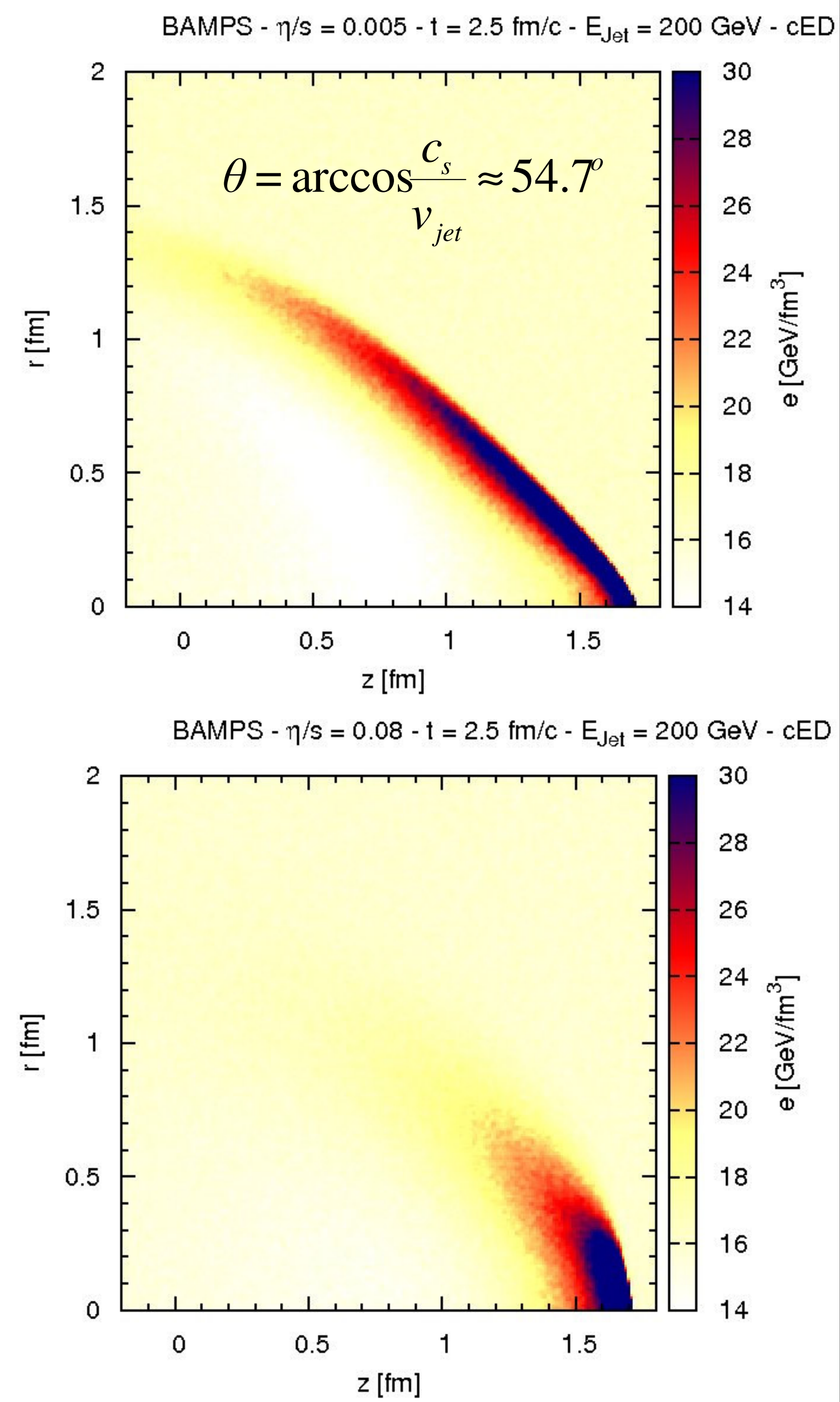

I. Bouras et al, arXiv:1201.5005 (2012)

BAMPS: GB Issues

- GB Matrix Element was a de-facto leading order 2->3 calculation (qq->qqg)

$$x = \frac{k_\perp}{\sqrt{s}} e^y$$

$$|\mathcal{M}_{qq' \to qq'g}|^2 \simeq 12 g^2 |\mathcal{M}_{qq \to qq'}|^2 (1-x)^2 \frac{q_\perp^2}{k_\perp^2 (\vec{q}_\perp - \vec{k}_\perp)^2}$$

- (1-x) dependence is usually dropped, GB interested in mid rapidity.
- Transport calculations need to cover the **full** rapidity range. Calculation becomes rather messy.
- Awaiting improved results

Exact Calculation removes forwards backwards peaks in rapidity (qq)

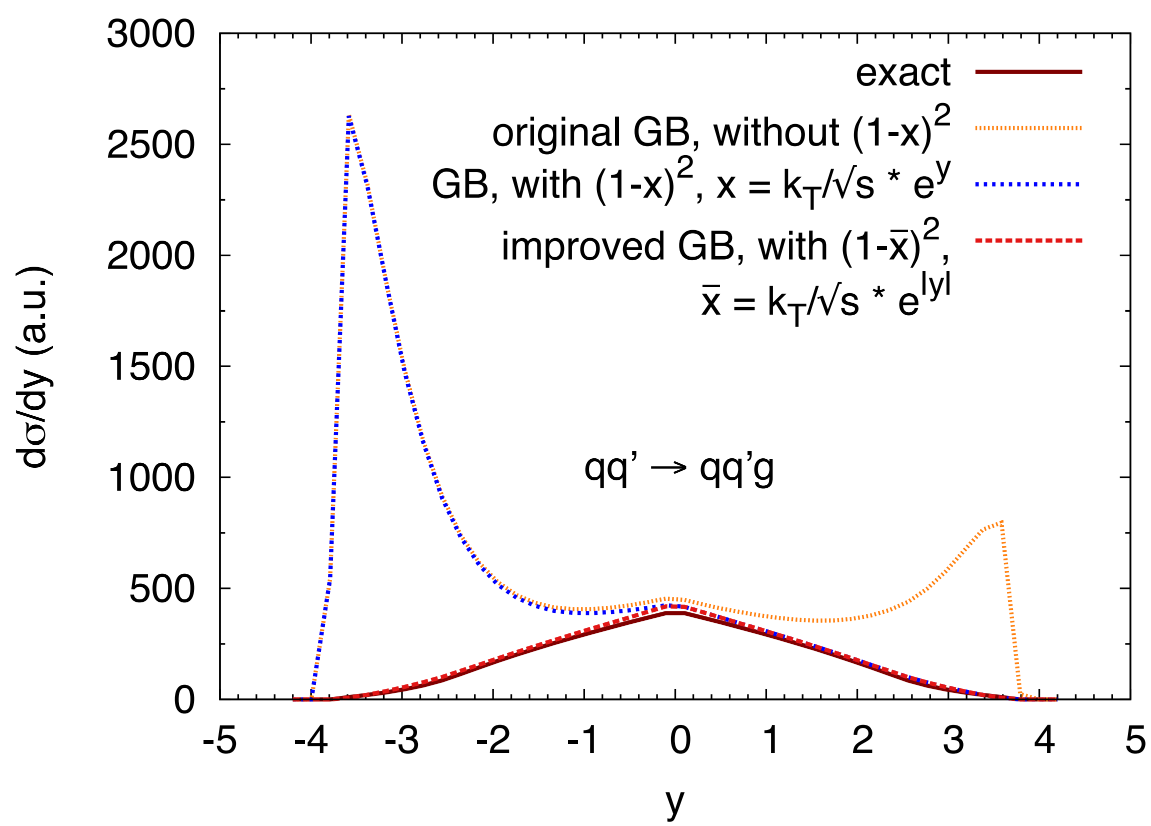

Total cross-section, integrals cutoff at Debye mass

Gunion.J & Bertsch.G, Phys.Rev.D**25** (1982)

GB Correction:
Fochler.O et al, hep-ph/1302.5250

Parton Cascades - VNI/BMS-2.0
Box Mode

Andong & VNI/BMS - Jet Transport

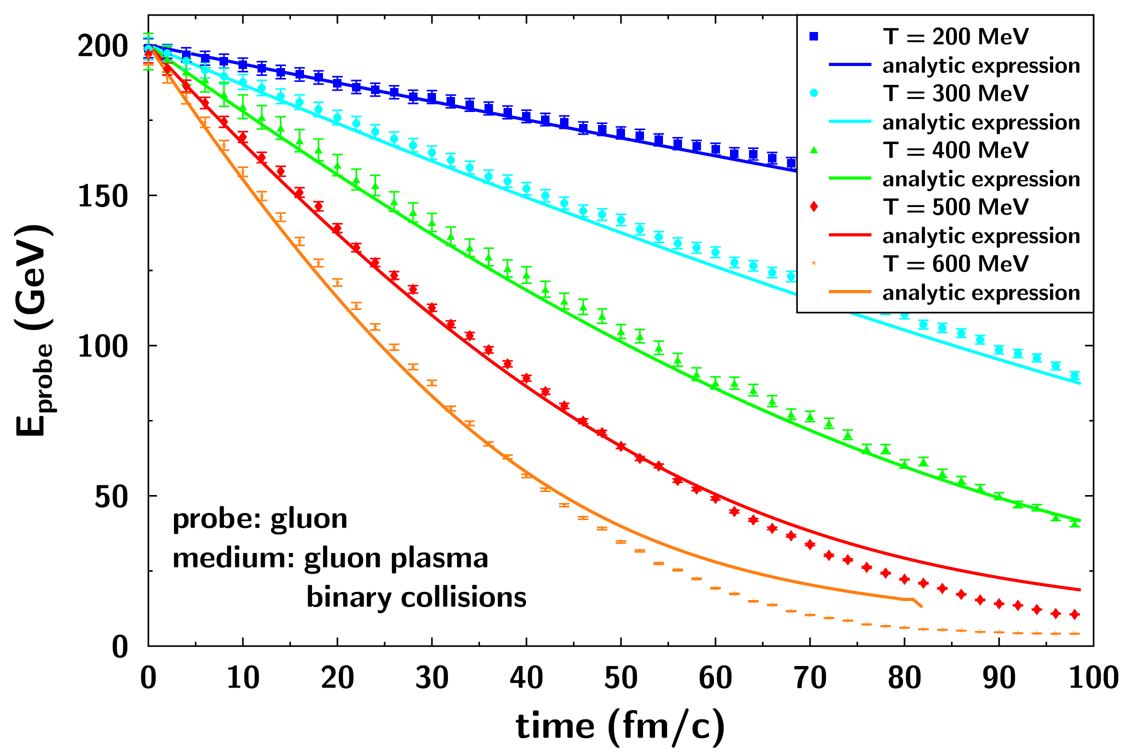

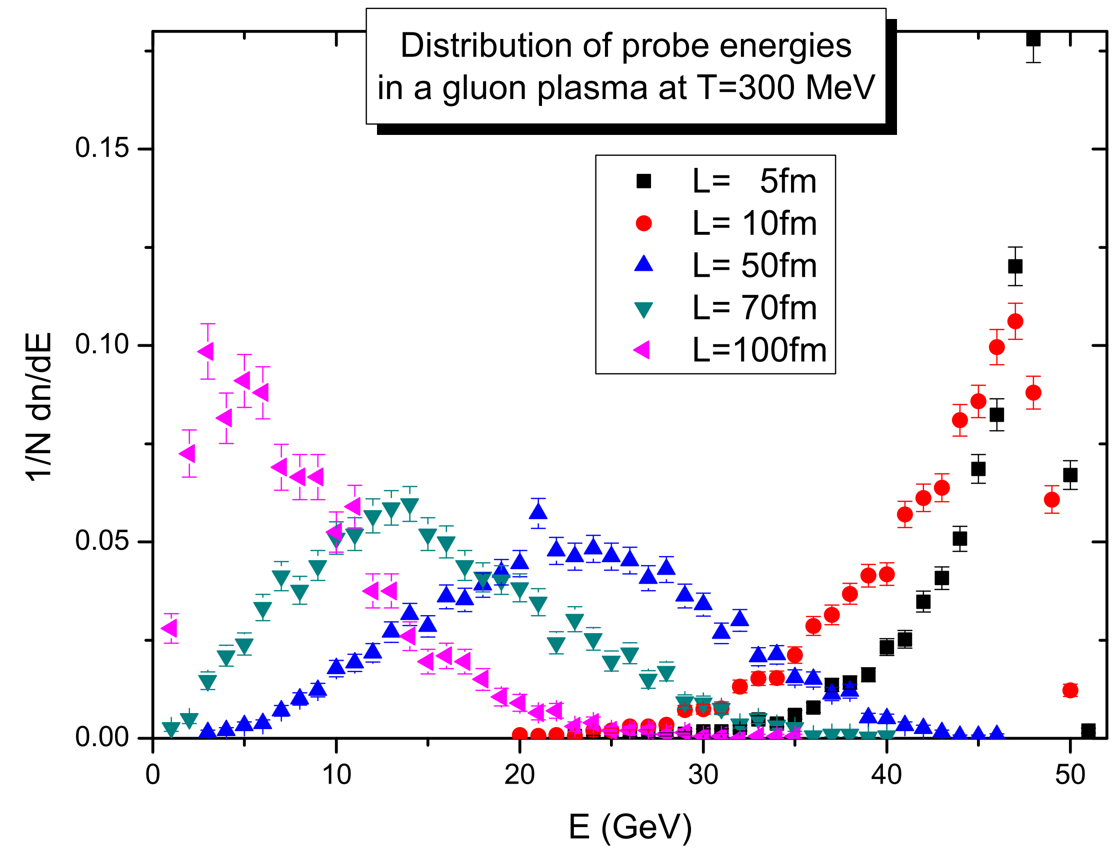

- First introduction of a box mode in VNI/BMS. Equilibrium thermal masses used to regularize cross-sections

- Compared the **elastic** energy loss of single quarks and gluons through a thermal box of idea pQGP matter

Shin, Bass, Müller. nucl-th/1006.1668 (2006)

Jet Simulation Method: Box Mode

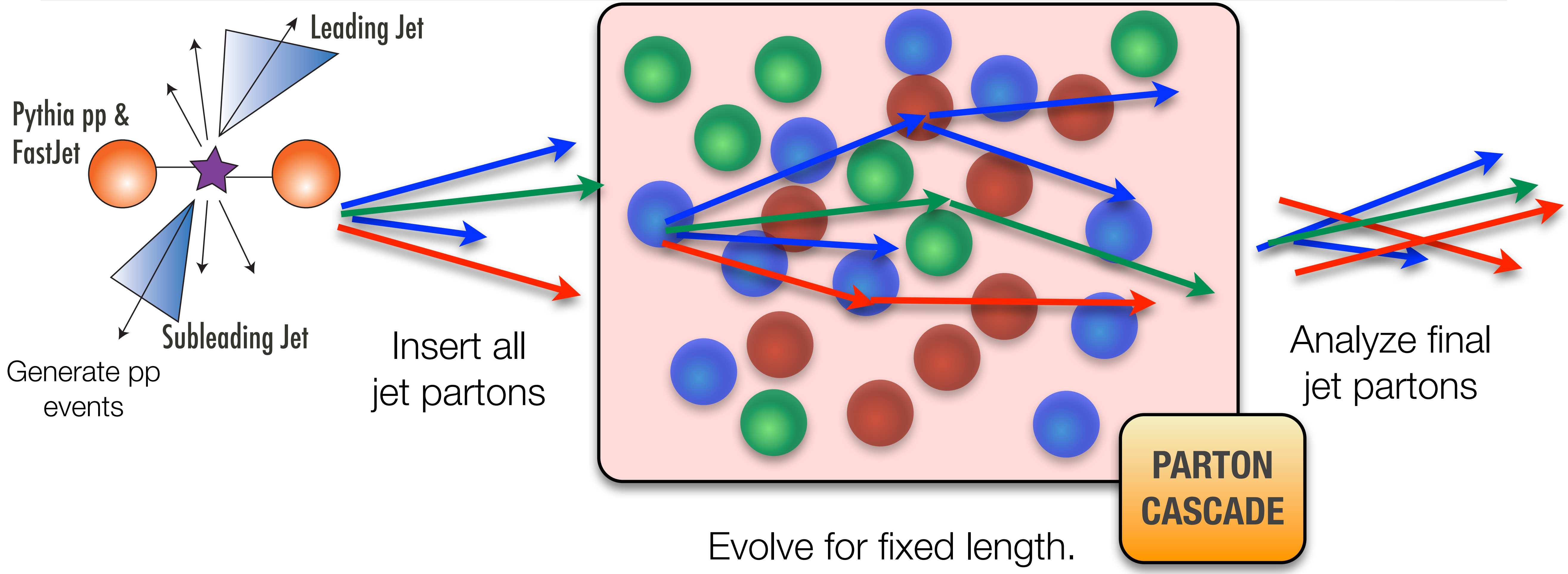

- Insert all partons from each jet into parton cascade box and evolve for a fixed path length.
- Medium is partonic and static, temperature can be fixed for the entire evolution.
- Medium and jet interact on an equal footing, track all resulting partons

A fully controllable brick of QCD matter

VNI/BMS - 2.0, a simple JET transport model

- Partonic transport via the Boltzmann equation. Treats medium and jet on an equal footing.

- Interactions are tree level 2->2 scatterings and final-state radiation. Radiation includes leading order (BDMPS-Z) LPM effect.

- Medium is a box of thermal partonic QGP at a fixed temperature. No expansion!

- Cross sections are screened by Debye mass, computed using the box temperature

- A generated jet is injected, cascade of interacting partons are tracked. Evolution of entire jet is recorded.

$$p^{\mu}\frac{\partial}{\partial x^{\mu}}F_k(x,\mathbf{p}) = \sum_{processes} \mathcal{C}_i F.$$

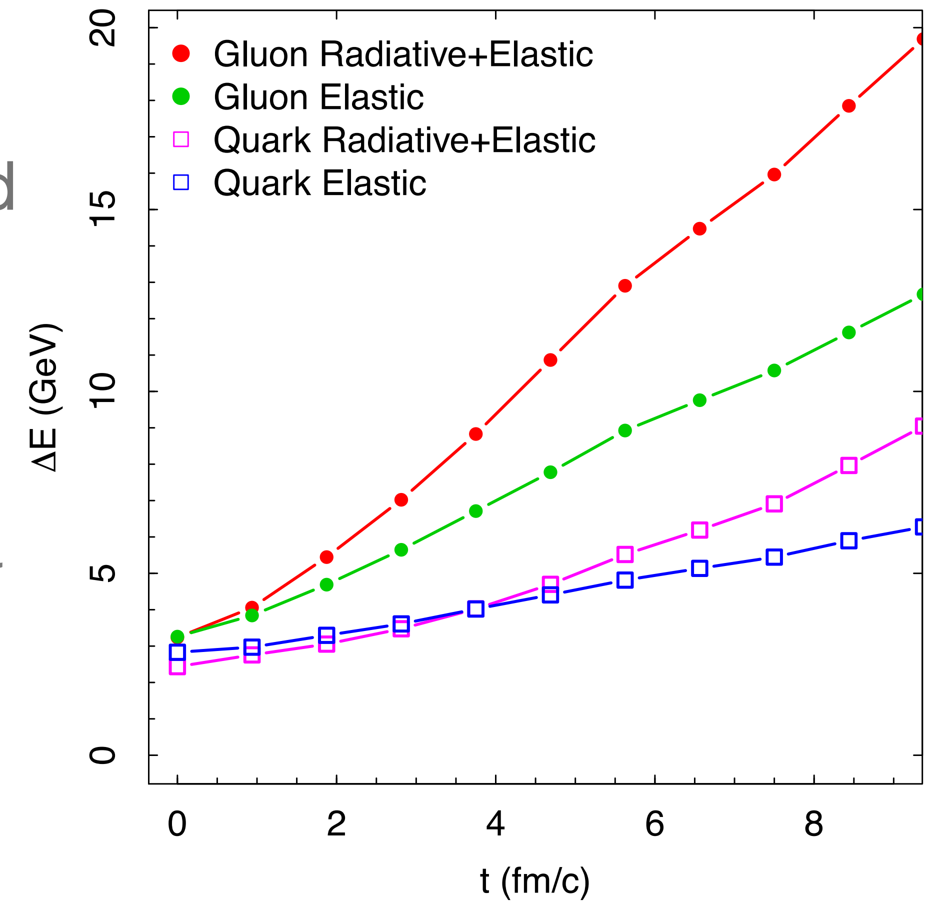

$$-\Delta E_{\mathrm{BDMPS}} = \frac{\alpha_s C_R}{8}\frac{\mu^2}{\lambda_g}L^2 \log\frac{L}{\lambda_g}.$$

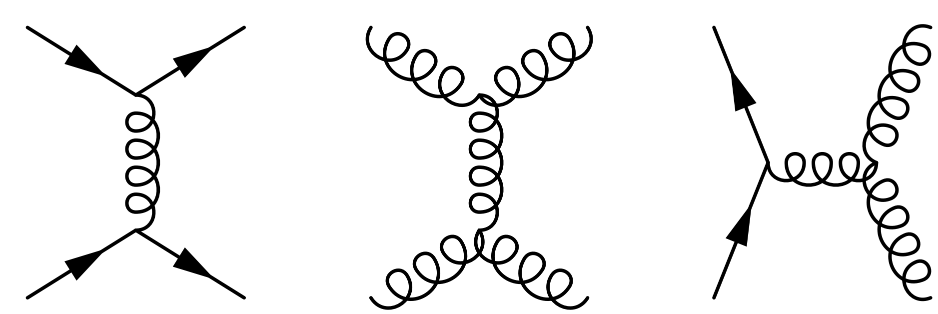

Zapp and Wiedemann, LPM Algorithm

- Probabilistic local implementation of coherence, gives rise to an L^2 energy loss.
- Post Inelastic scattering, compute formation time of emitted gluon
    - Emitting parton does not interact during this time
    - Radiated gluon rescatters elastically off the medium, recompute modified formation time
    - Repeat until formation time expires
    - Quark and gluon propagate freely
- Simulates coherent emission from multiple centers

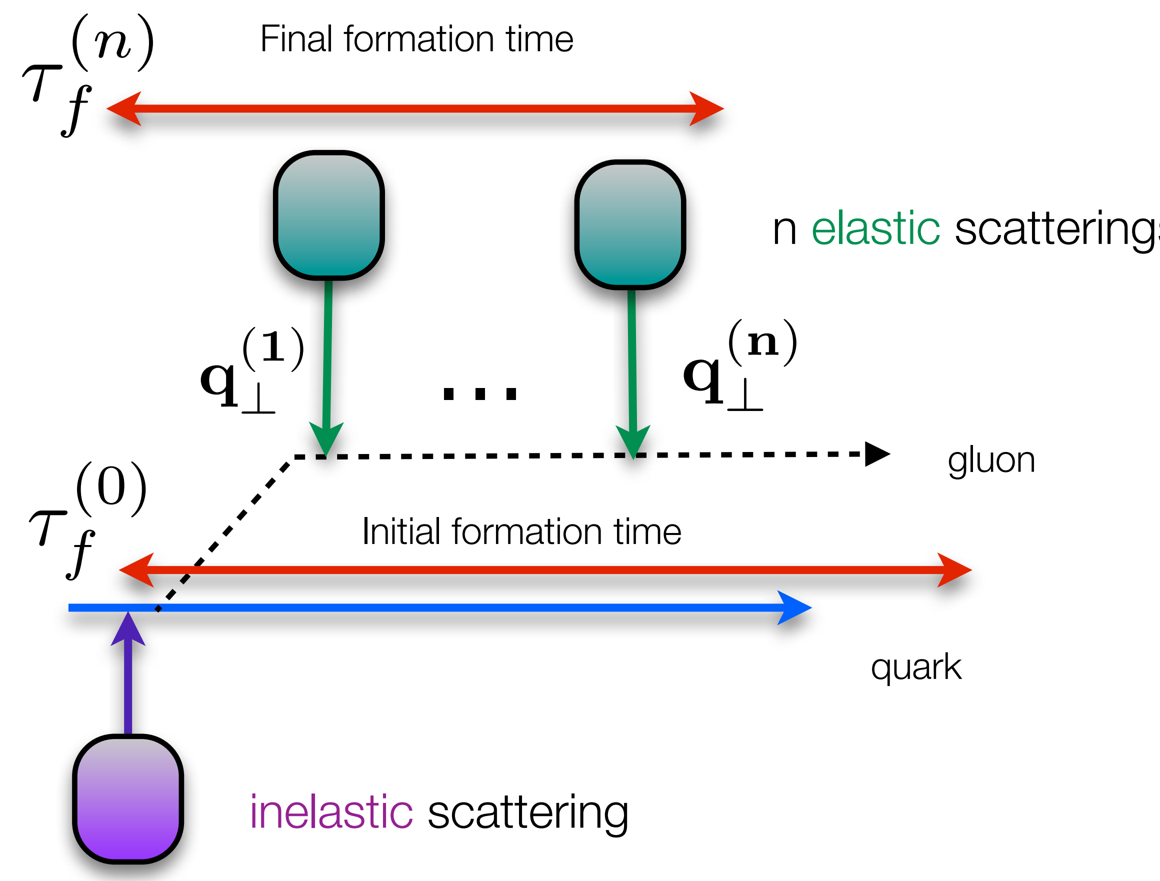

$$\tau_f^{(n)} = \frac{2\omega}{\left(\mathbf{k}_\perp + \sum_{i=0}^{n} \mathbf{q}_\perp{}^{(i)}\right)^2}$$

Zapp K, Wiedemann U. *Phys Rev Lett,* 103 (2009) JEWEL
CCS, S.A.Bass, D.K.Srivastava, *hep-ph/1101.4895*

Hadronization In VNI/BMS - 2.0

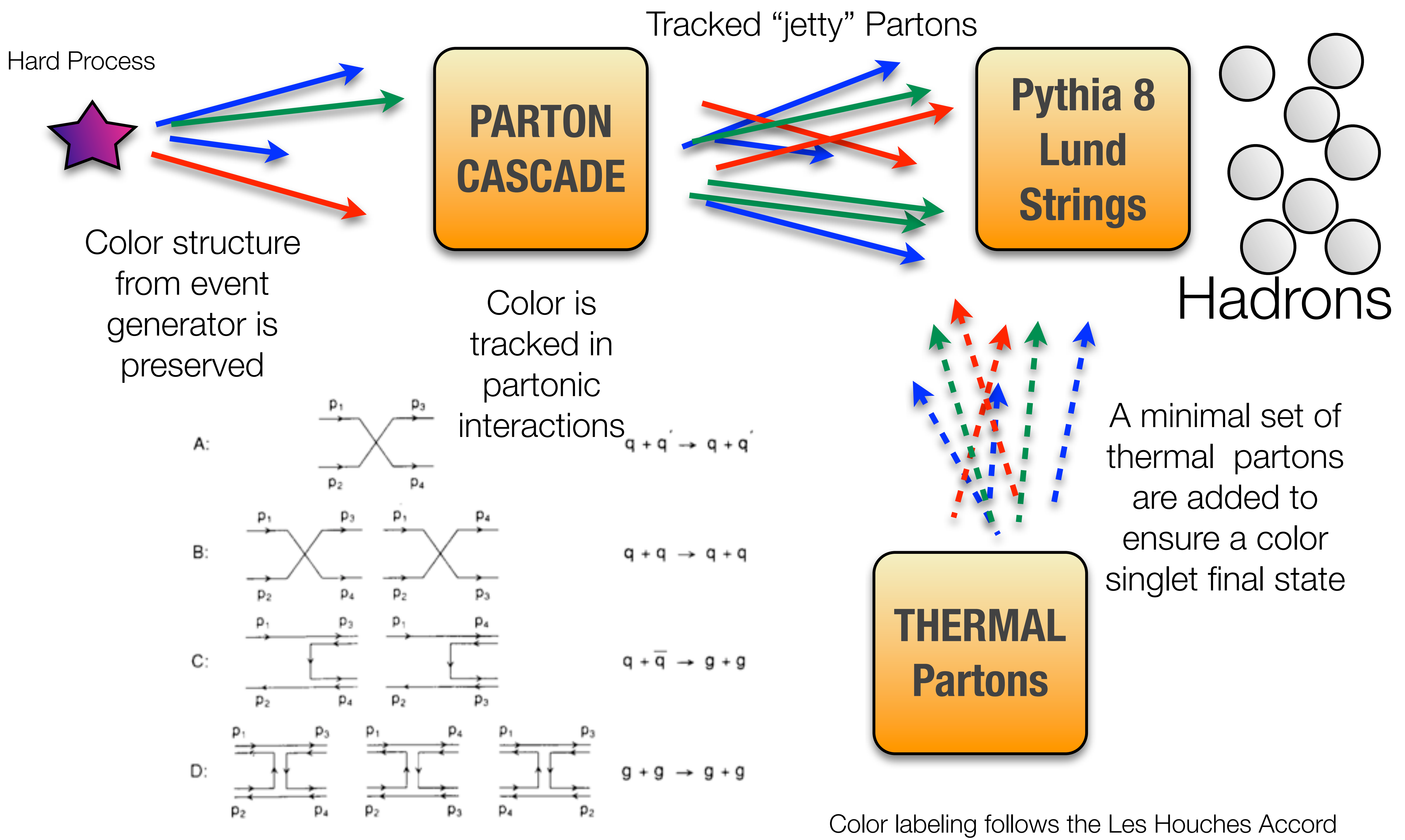

Hadronization In VNI/BMS

100 GeV quark evolved for 4fm in a box at T=350 MeV

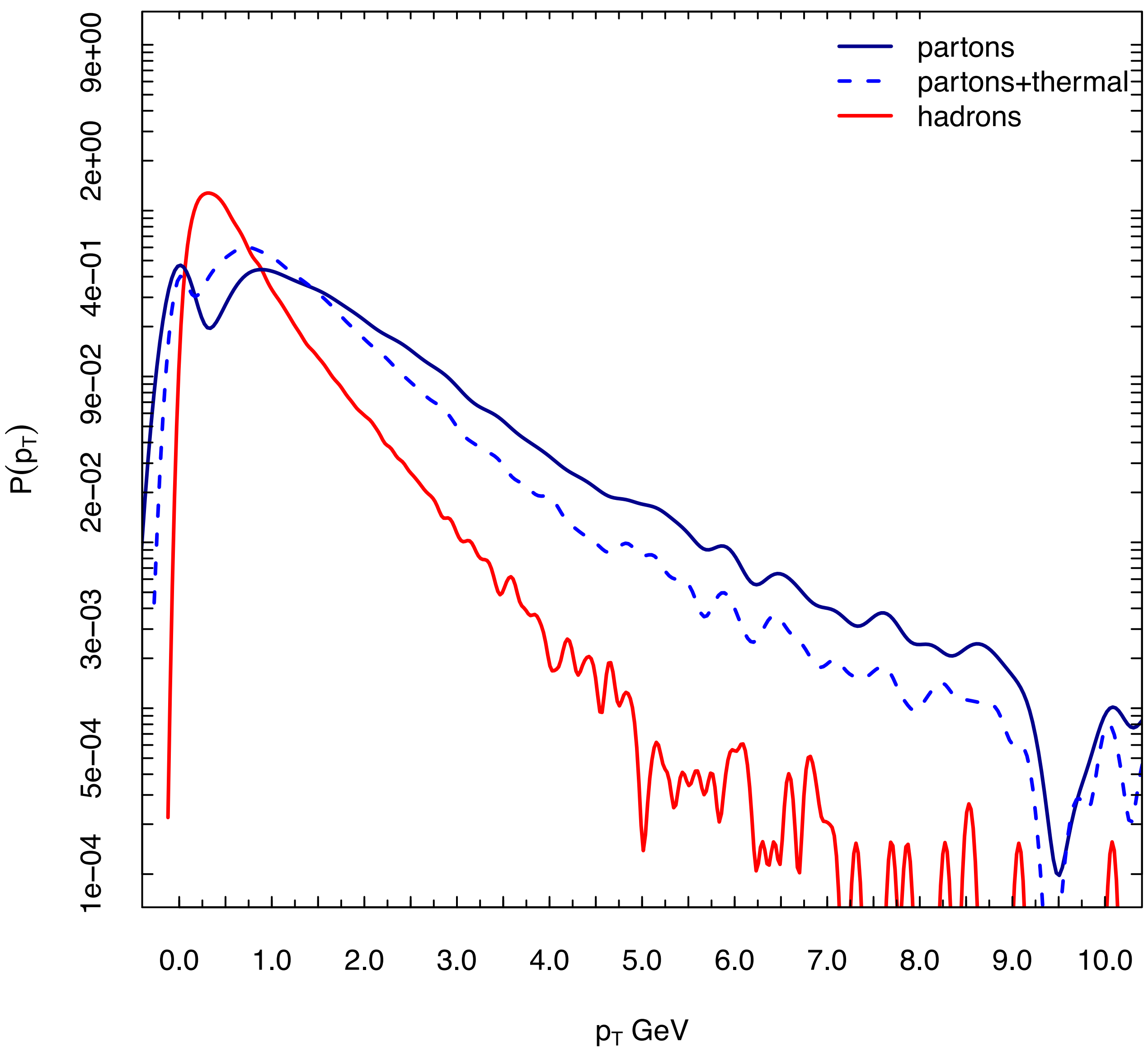

Hadronization contracts the transverse momentum distribution

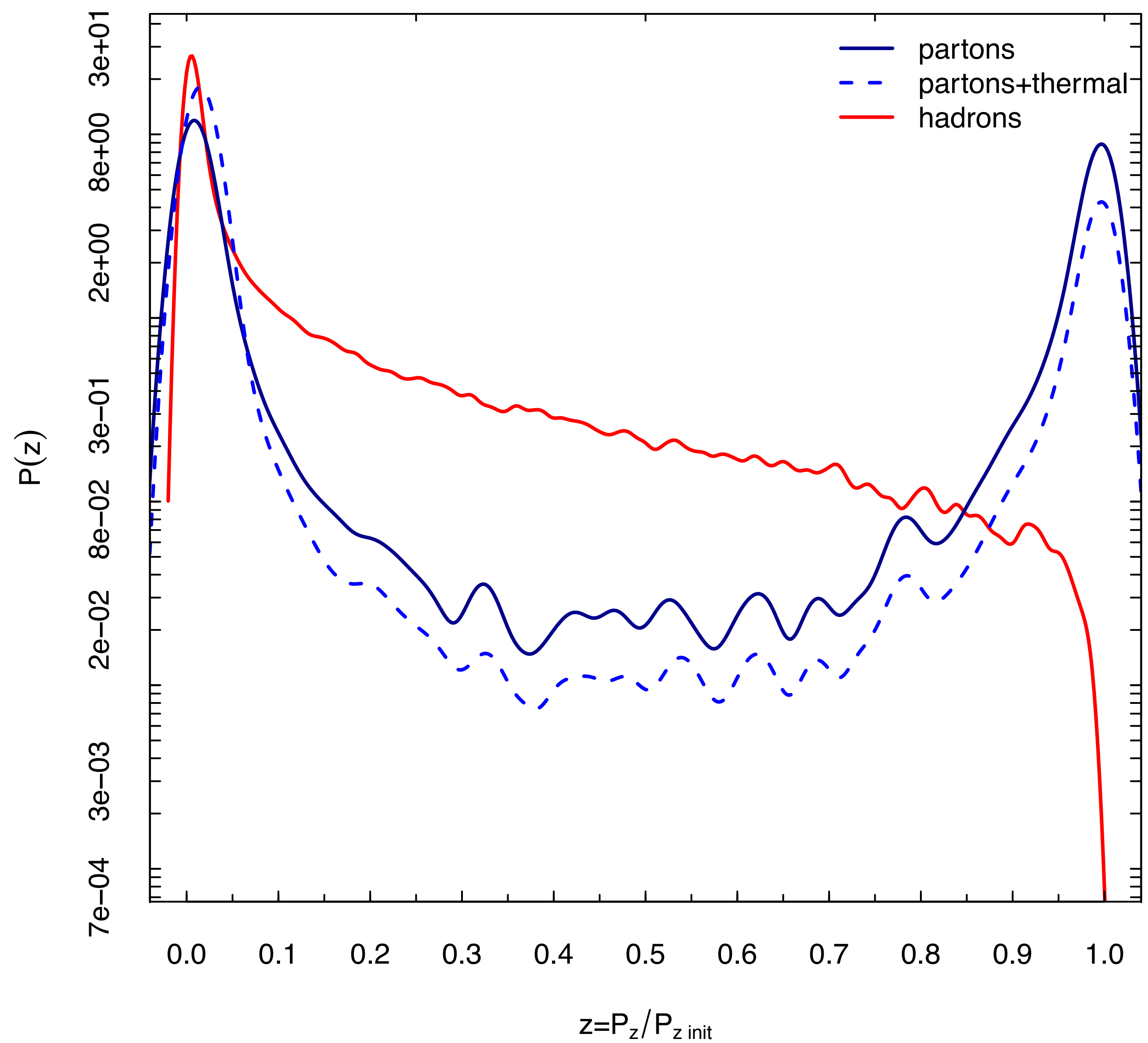

Hadronization smooths the longitudinal distribution, peak at Z=1 is redistributed

Jet Observables - VNI/BMS - Box Mode

LHC Dijet Results

Circle Mode + Glauber Vertices can reproduce LHC data reasonably well.

Central collisions (0-10%)

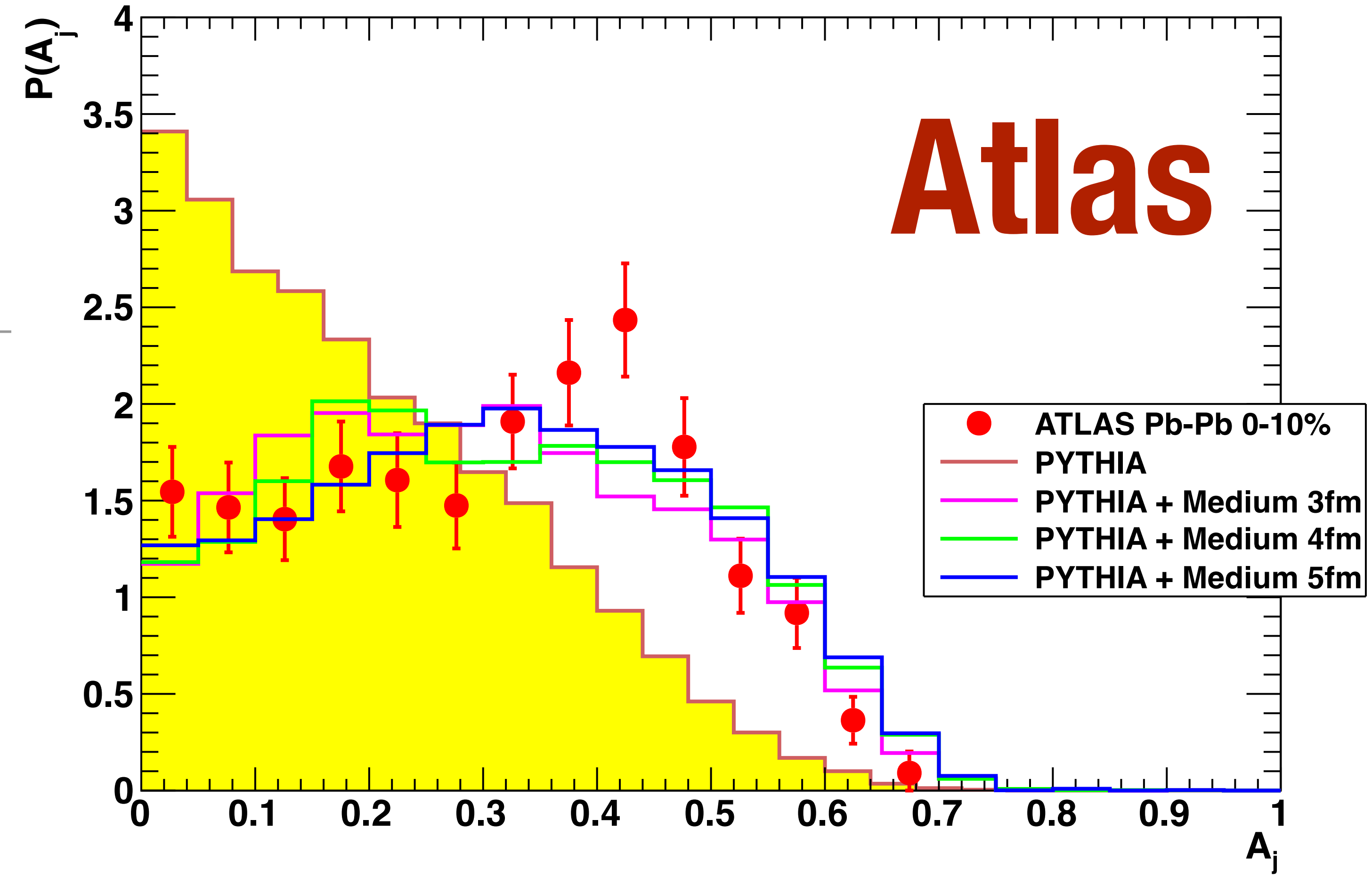

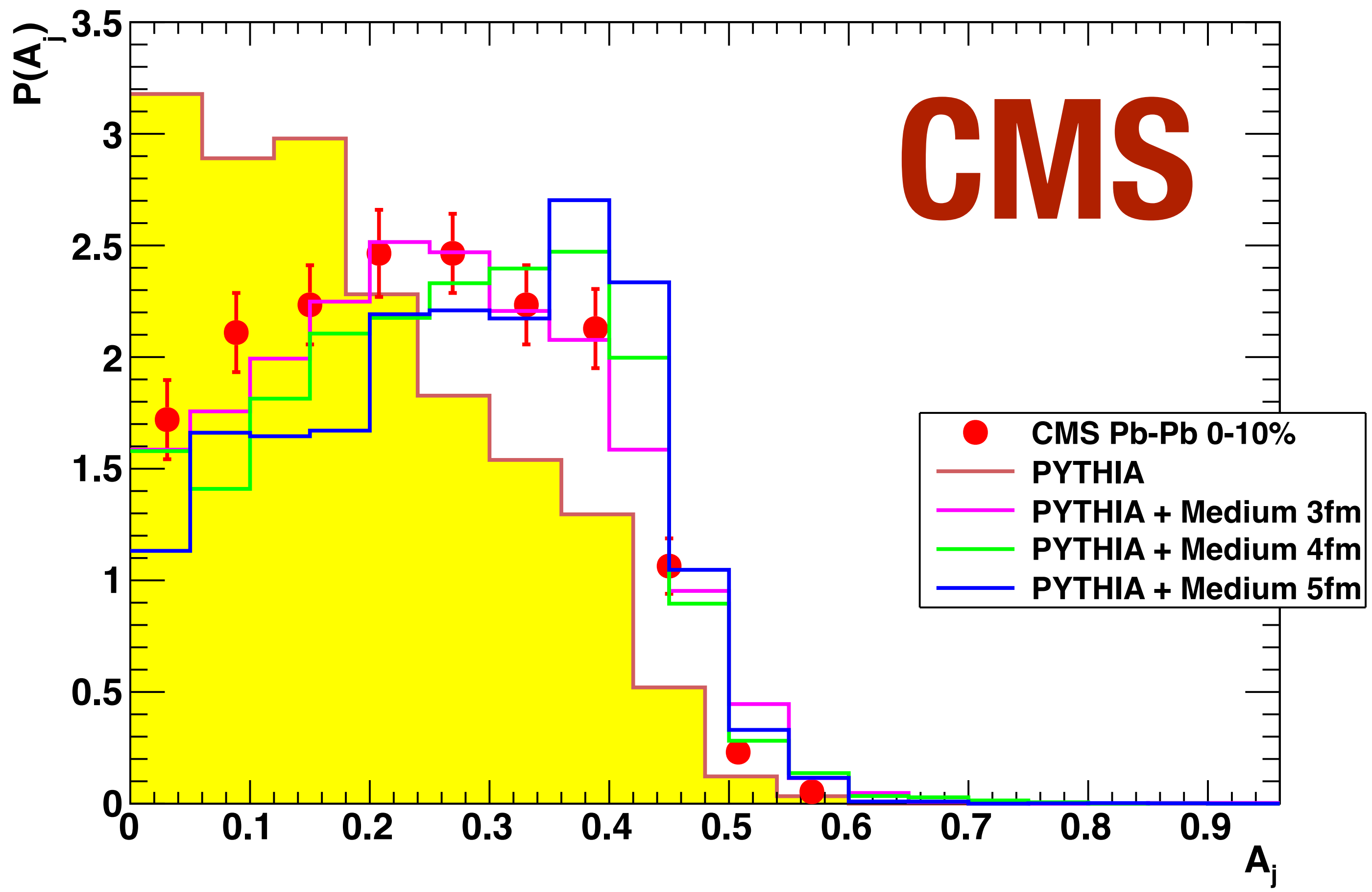

Both results include detector smearing effect

$$E_t^\star \sim N(E_t, \alpha\sqrt{E_t}), \quad \alpha \simeq 1.2$$

Presented at QM 2011

Process Dependence

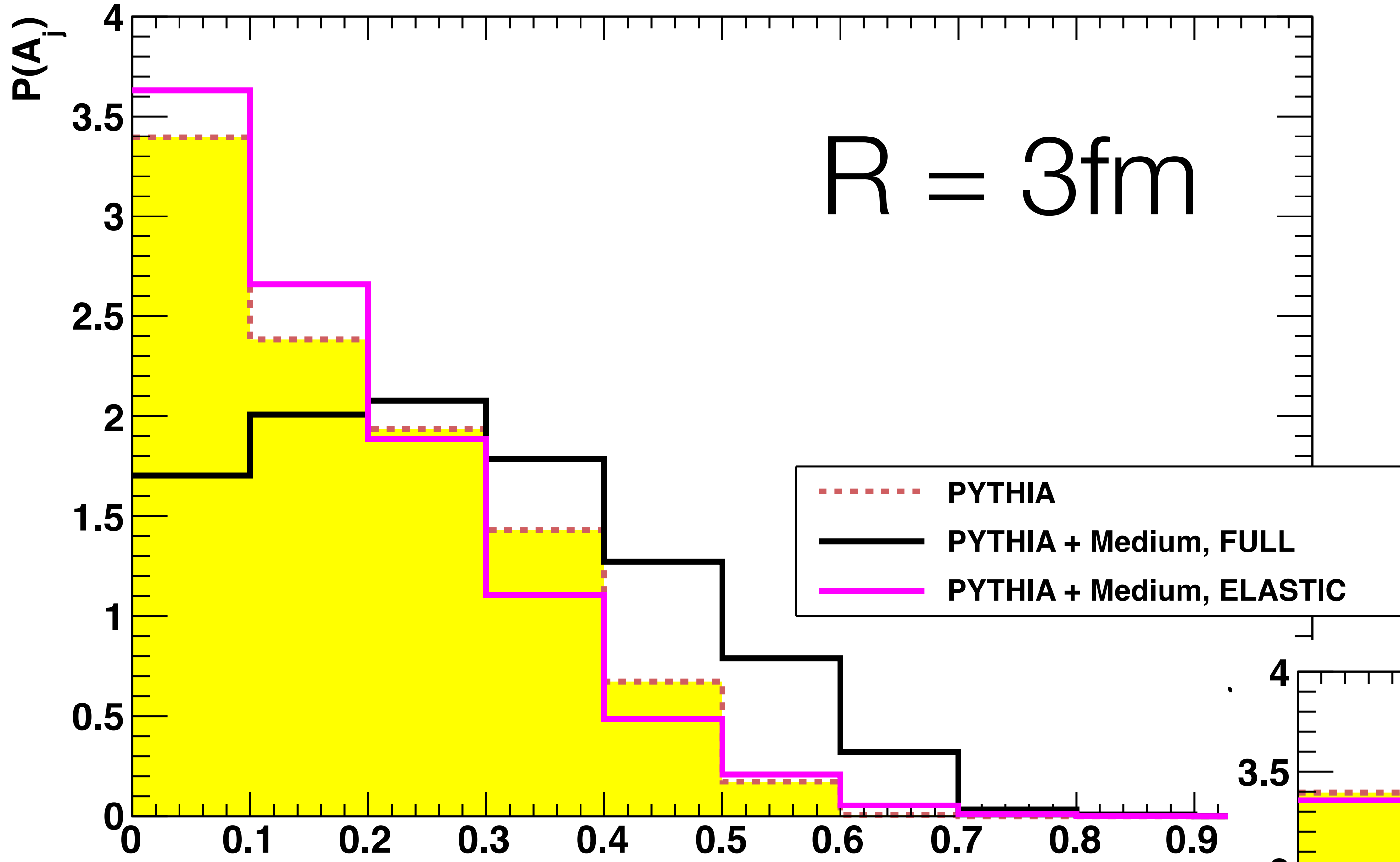

- T = 0.35 GeV
- Elastic only, distribution shifts to the left. Medium reduces the asymmetry
- Jet "picks up" medium particles by forward scattering

$E_{T1} > 100\text{GeV} \quad E_{T2} > 25\text{GeV}$

Radiation plus elastic gives increased asymmetry.

Soft radiated gluons can be elastically scattered out of the jet cone

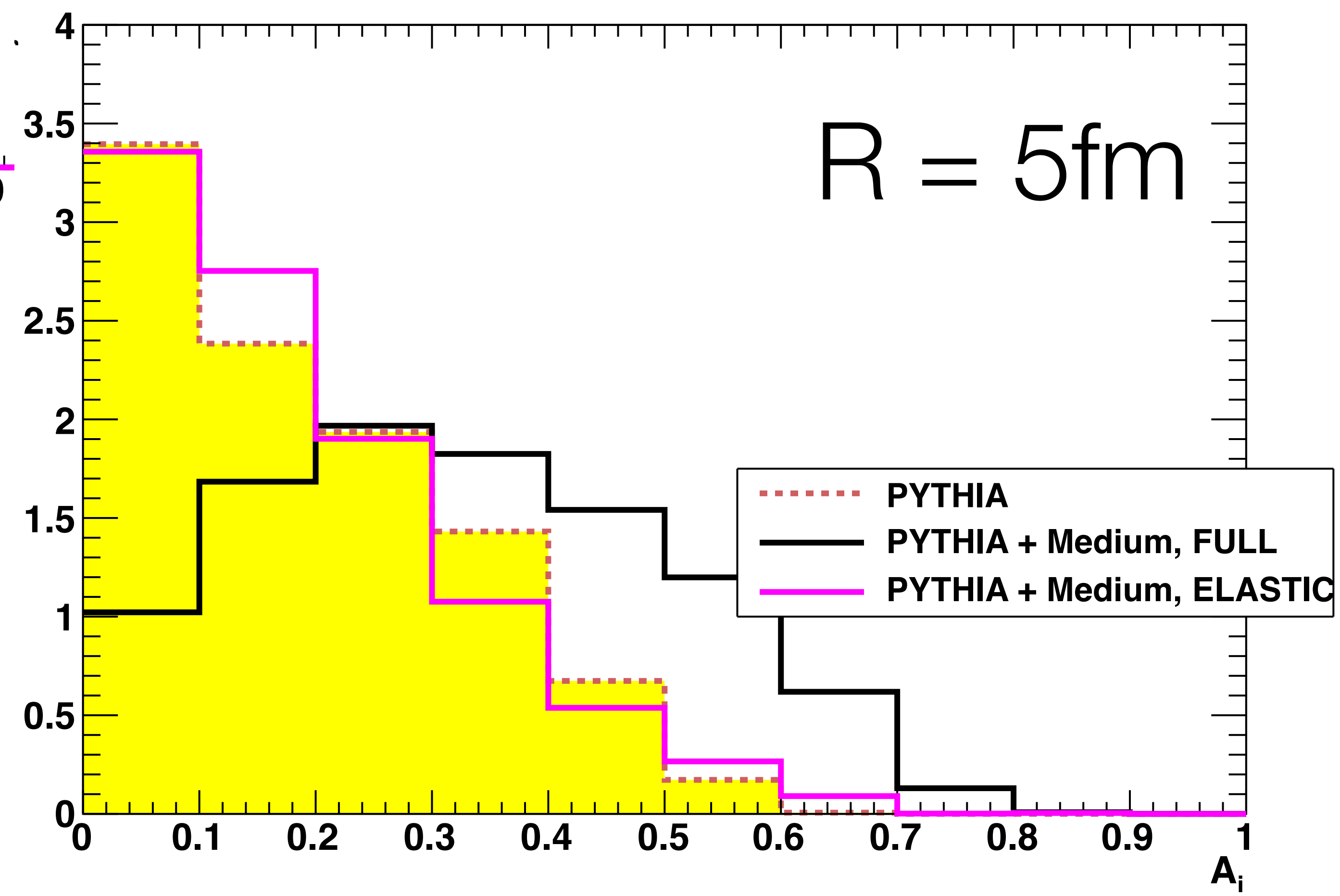

Temperature Dependence

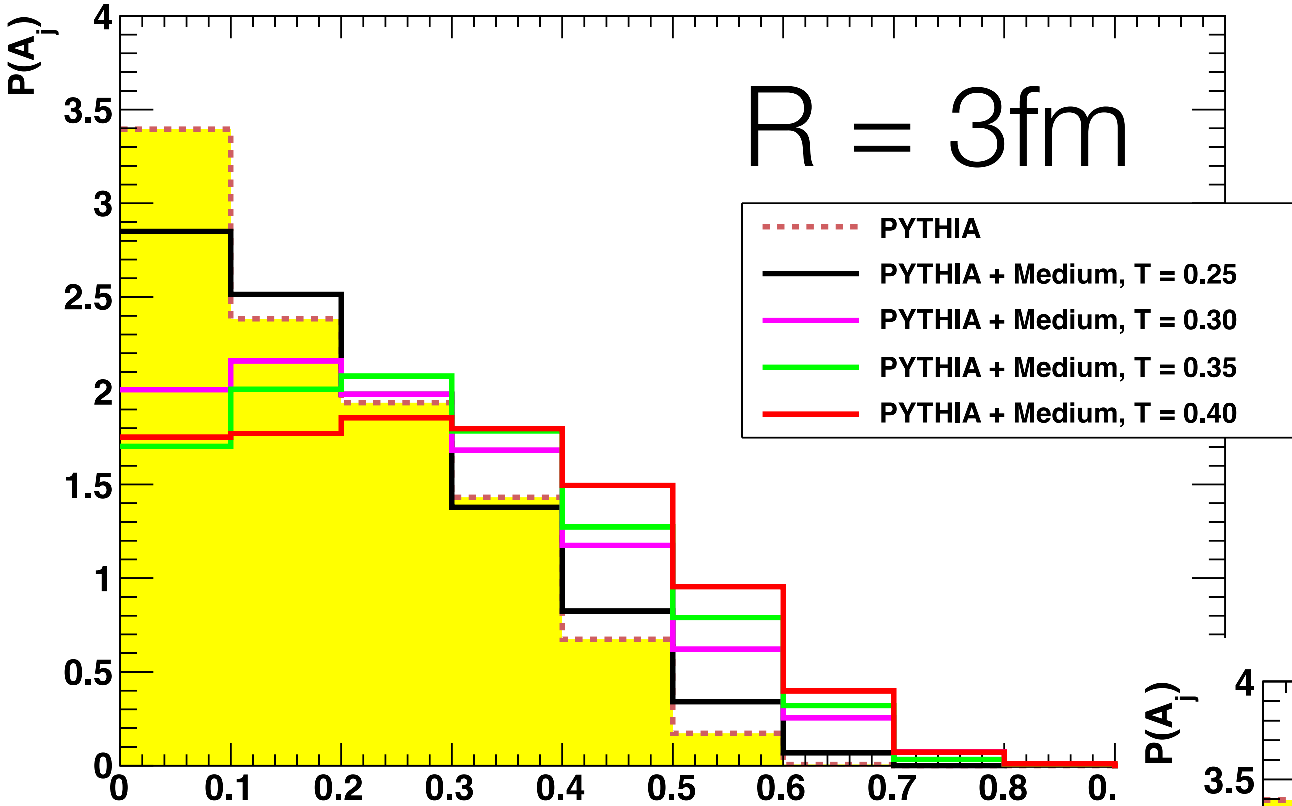

- Medium temperature controls:
  - Debye screening length
  - Minimum pt cutoff
  - Medium density

$E_{T1} > 100\text{GeV} \quad E_{T2} > 25\text{GeV}$

T(MeV)	$\hat{q}$ (GeV^2/fm)
250	1.125
300	1.5
350	2.125
400	3.0

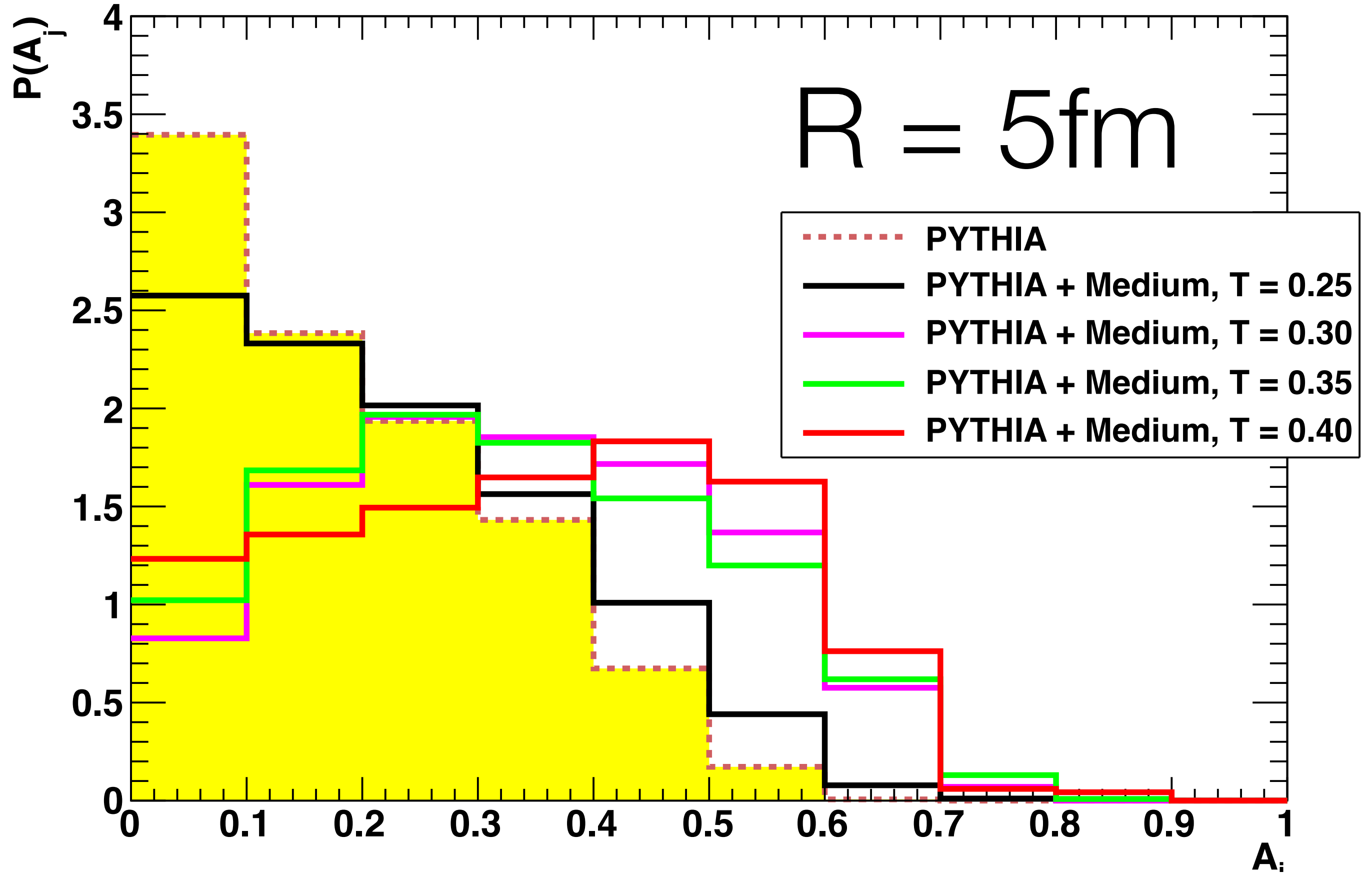

RHIC Dijet Asymmetry - Varying Strong Coupling

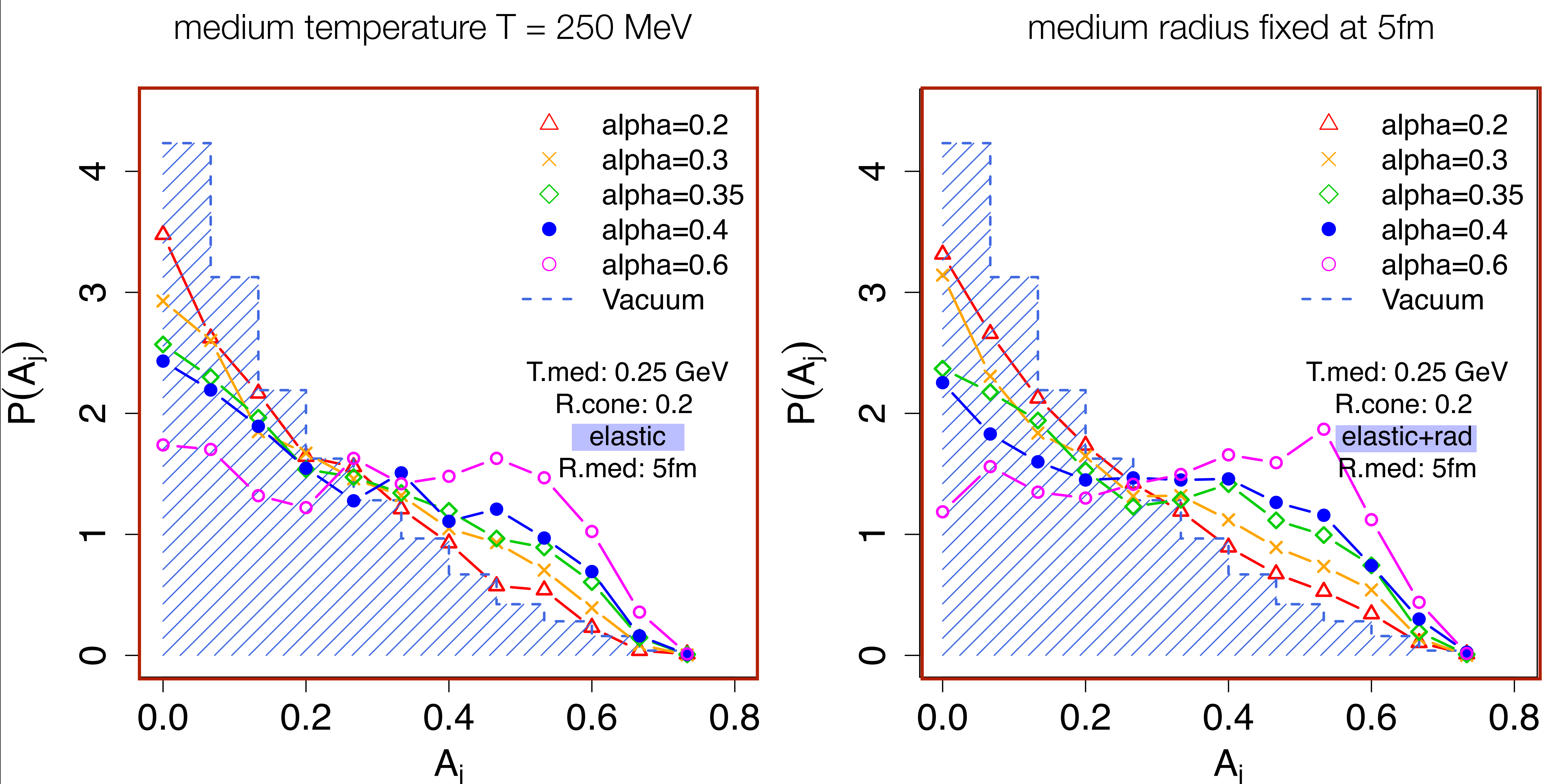

Increasing Strong Coupling increases asymmetry

C.C-S, B.Müller, "What can we learn from Dijet suppression at RHIC", Phys.Rev.C 86 (2012)

RHIC - Jet Shape

Reconstruct jets with Anti-Kt at successively larger cone radii

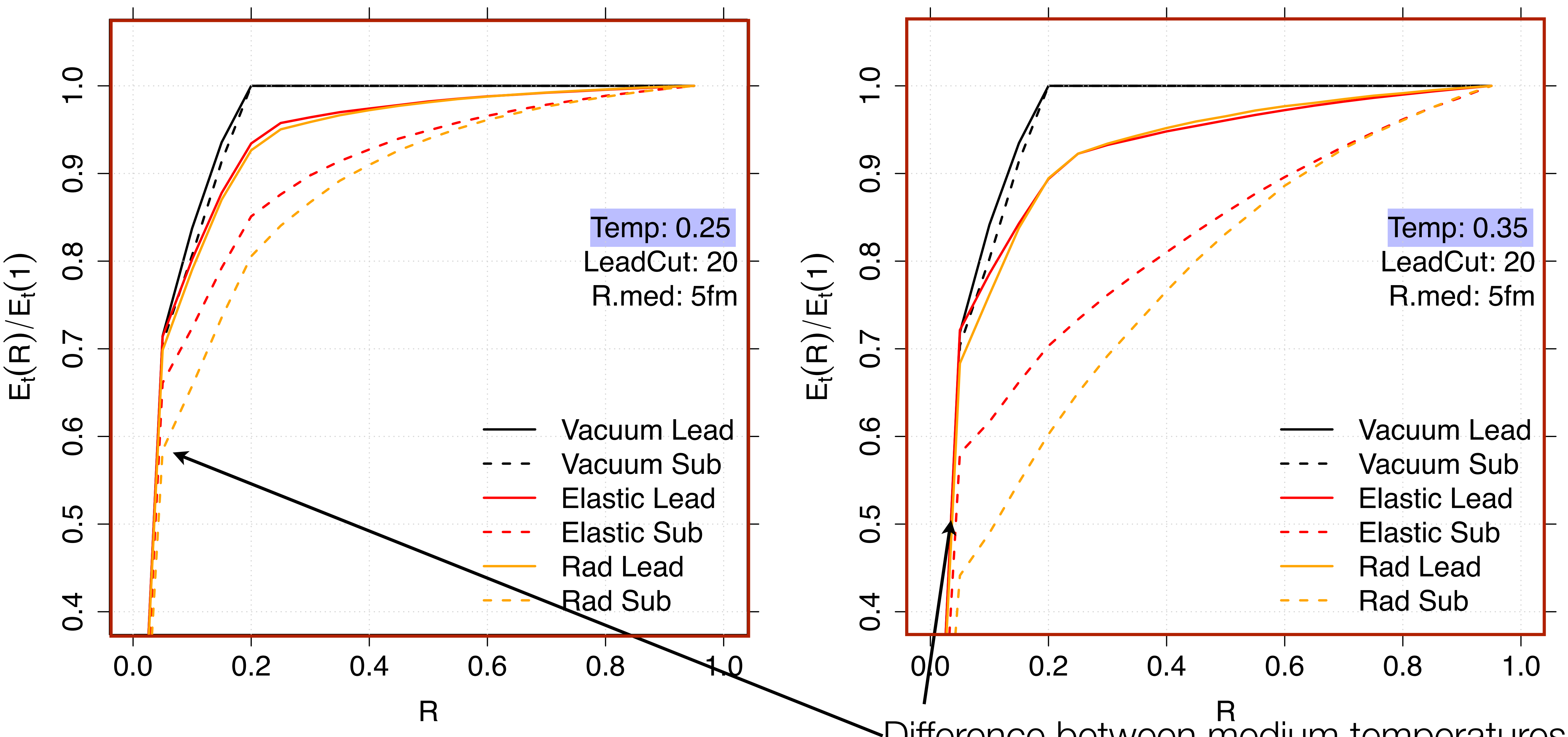

Clear separation between elastic (red) and radiative (orange) modes

C.C-S, B.Müller, "What can we learn from Dijet suppression at RHIC", Phys.Rev.C 86 (2012)

Jet Fragmentation - Longitudinal

$$z = E_T/E_{T,Jet} \cos \Delta R$$

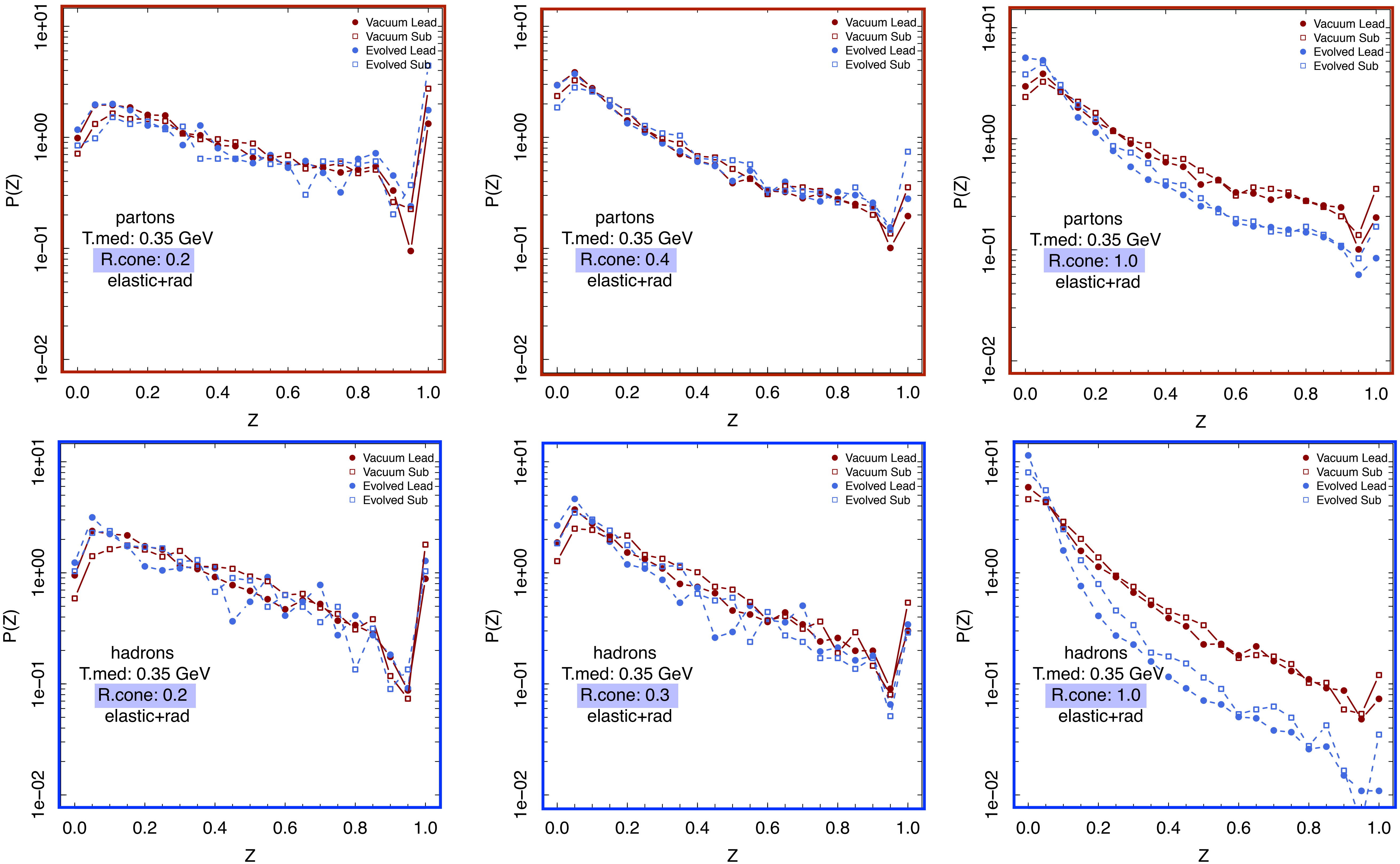

CMS Photon - Jet Correlation

CMS hep-ex/1205.0206

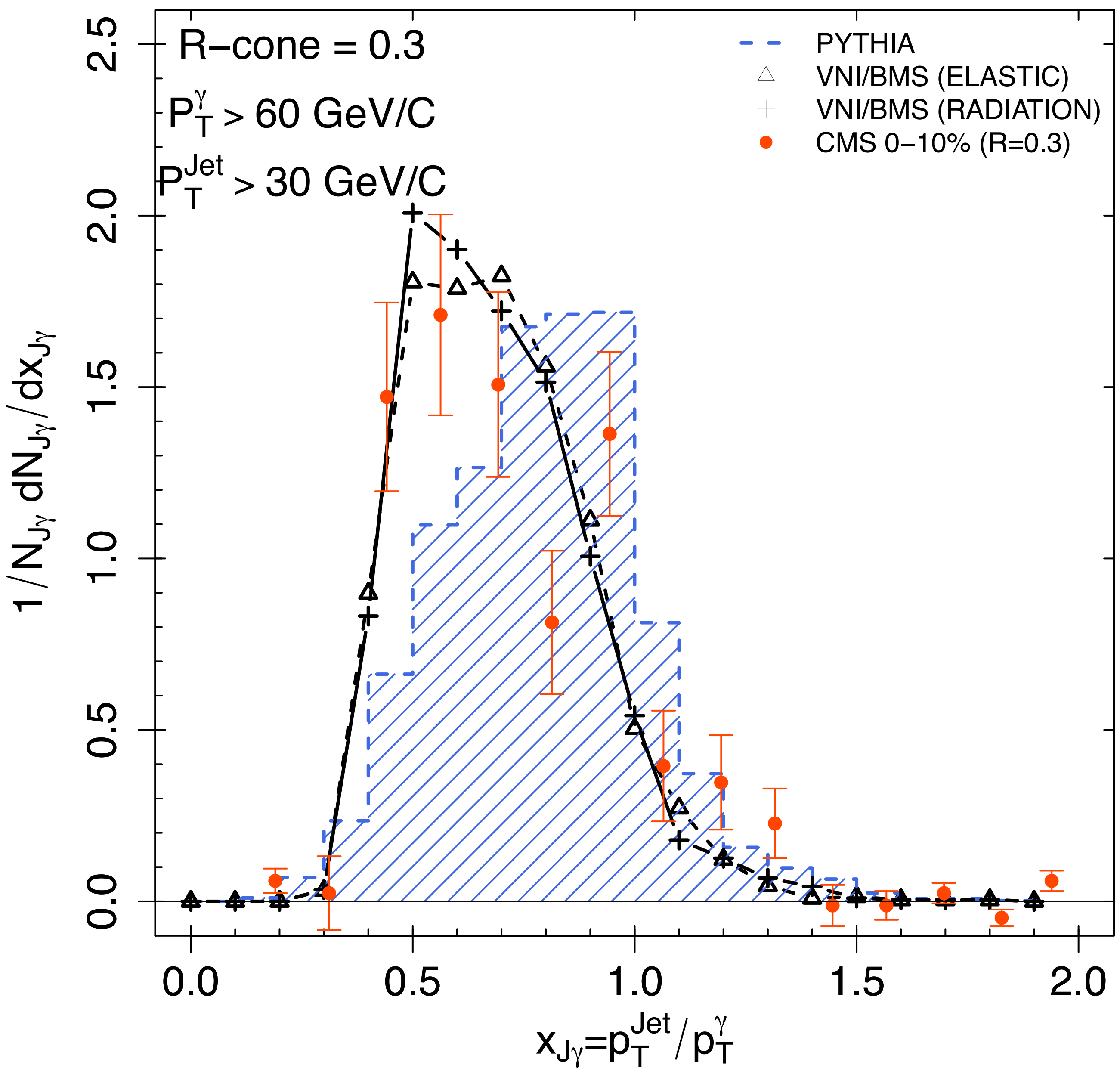

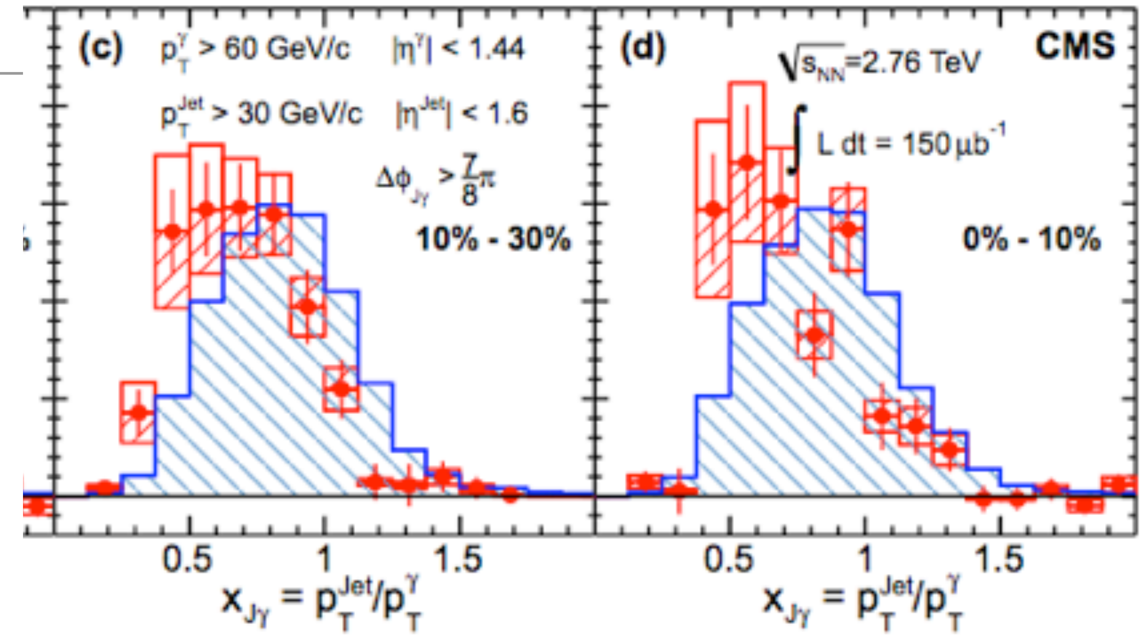

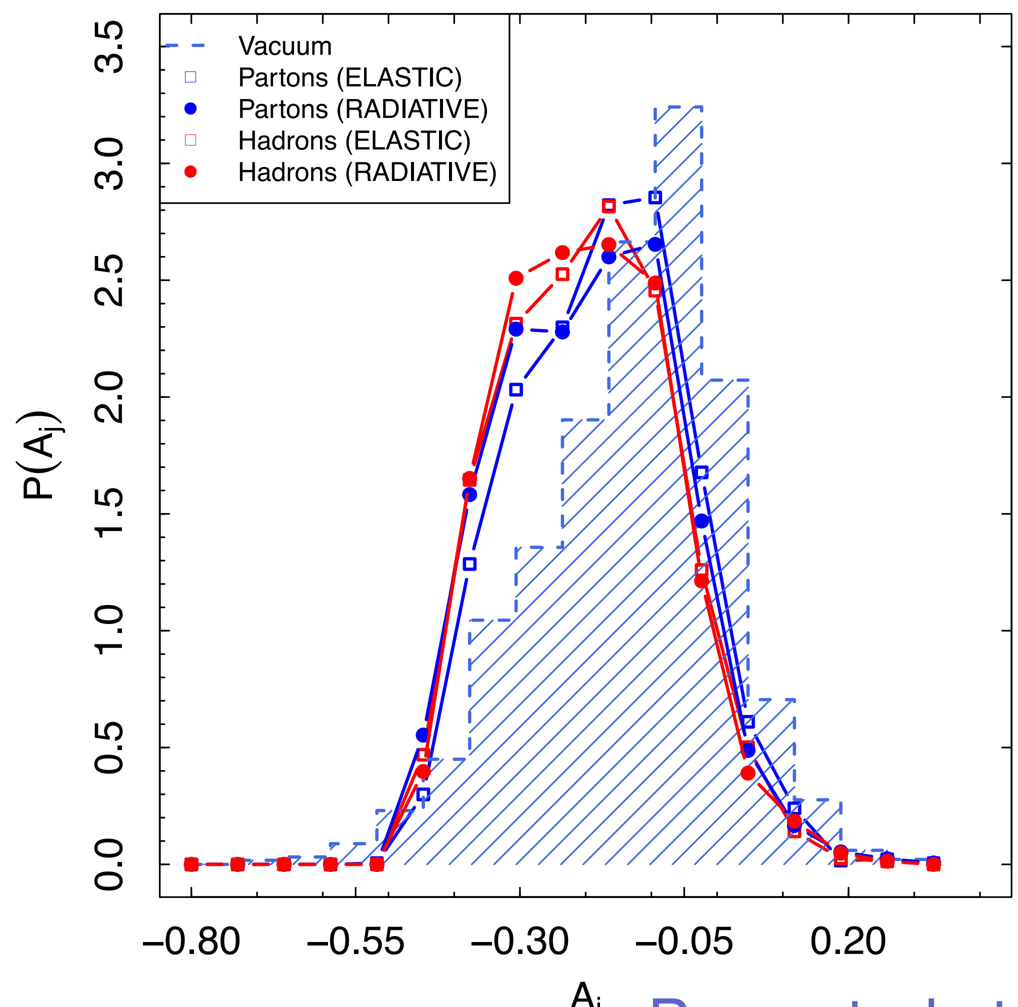

$$E_{T,\gamma} > 60\text{GeV}$$
$$E_{T,\text{Jet}} > 30\text{GeV}$$

$$A_j = \frac{E_{T,jet} - E_{T,\gamma}}{E_{T,jet} + E_{T,\gamma}}$$

Presented at QM 2012

Thermal Masses for medium partons

- Previous results from VNI/BMS derived from a medium of massless partons

- Interaction cross-sections are always screened by the Debye mass $$m_D^2 = \frac{1}{6}(2N_c + N_f)g^2T^2$$

- Introduce asymptotic HTL masses for medium partons

$$m^2 = kg^2T^2, \quad k = \begin{cases} \frac{1}{6}N_c + \frac{1}{12}N_f & \text{gluon} \\ \frac{1}{4}C_F & \text{quark} \end{cases}$$

- Introduce a dimensionless scaling parameter μs to 'dial' medium masses

$$m^2 = k\mu_s^2 g^2 T^2.$$

- NB: Medium number density now scales with masses

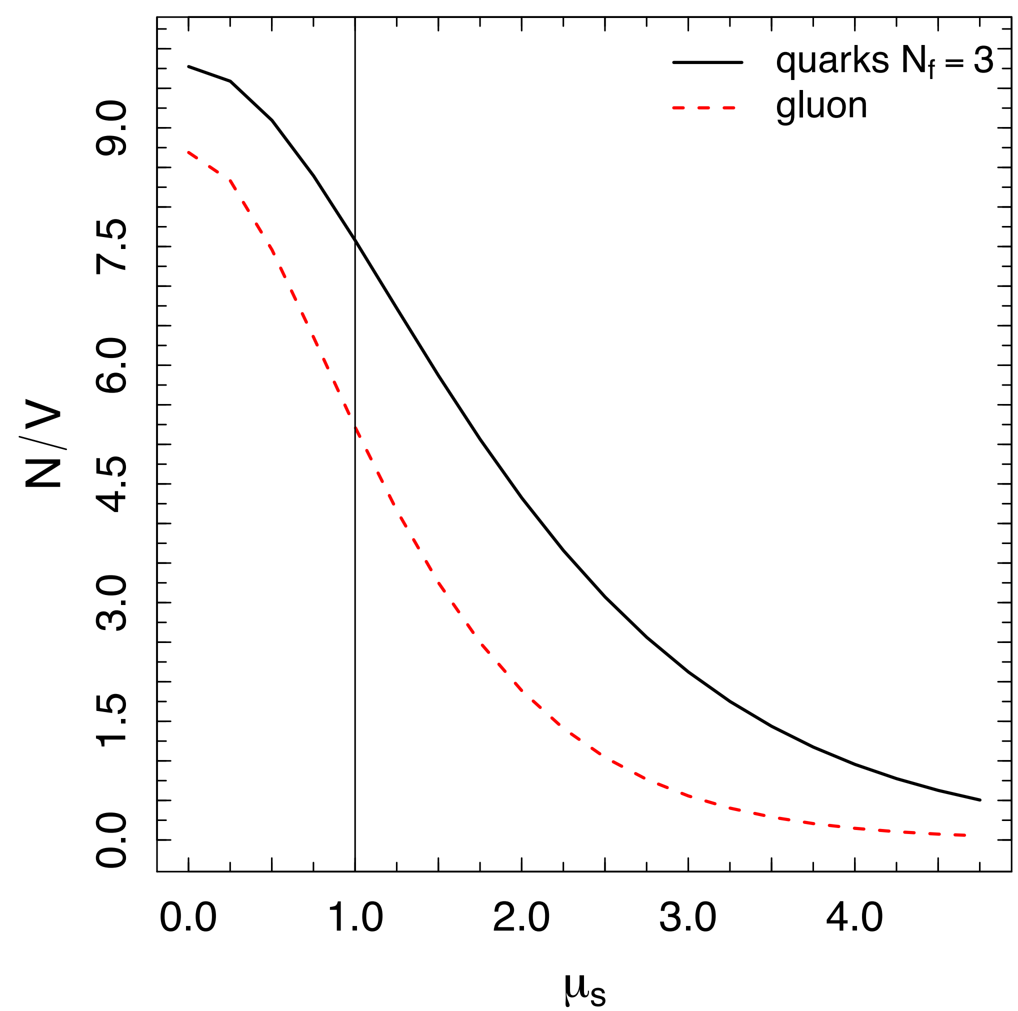

$$\frac{N}{V} = \frac{gTm^2}{2\pi^2}K_2(\frac{m}{T})$$

Measuring Transport Coefficients in VNI/BMS

- Fix medium temperature T=350 MeV, run code without radiation or hadronization.

- Run events with quark probes at fixed energies

- Extract q-hat and e-hat from transverse momentum and energy loss accumulated by the probe

$$\hat{q} = \frac{1}{L} \sum_{i=1}^{N_{\rm coll}} \Delta p_{T,i}^2. \qquad \hat{e} = \frac{1}{L} \sum_{i=1}^{N_{\rm coll}} \Delta E_i ,$$

- For light probes in a massless medium we expect from pQCD calculations

$$\hat{q}(T) = 4\pi C_R \alpha_s^2 \mathcal{N}(T) \ln\left(\frac{q_{\rm max}^2}{m_D^2} + 1\right),$$

$$\mathcal{N}(T) = \frac{\zeta(3)}{\pi^2}\left(2N_c + \frac{3}{2}N_f\right)T^3,$$

$$\hat{e}(T) = \frac{4\pi\alpha^2 T^2}{3}\left(1 + \frac{N_f}{6}\right)\ln\left(\frac{ET}{m_D^2}\right)$$

Elastic Energy Loss

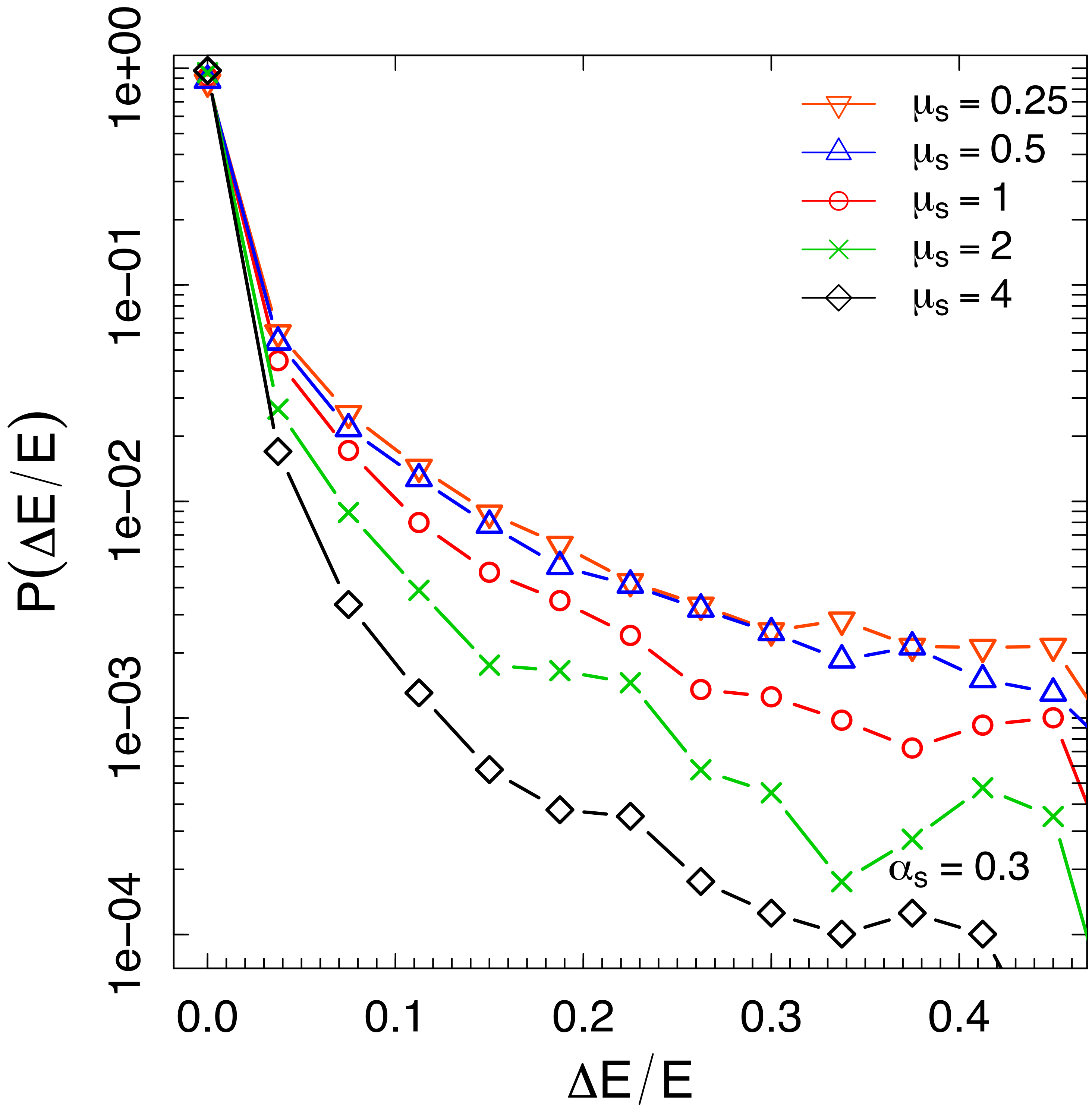

Confirms kinematic intuition, higher medium constituent masses recoil less resulting in a lower energy loss

T=350 MeV, Alpha = 0.3

Q-hat / E-hat Ratio

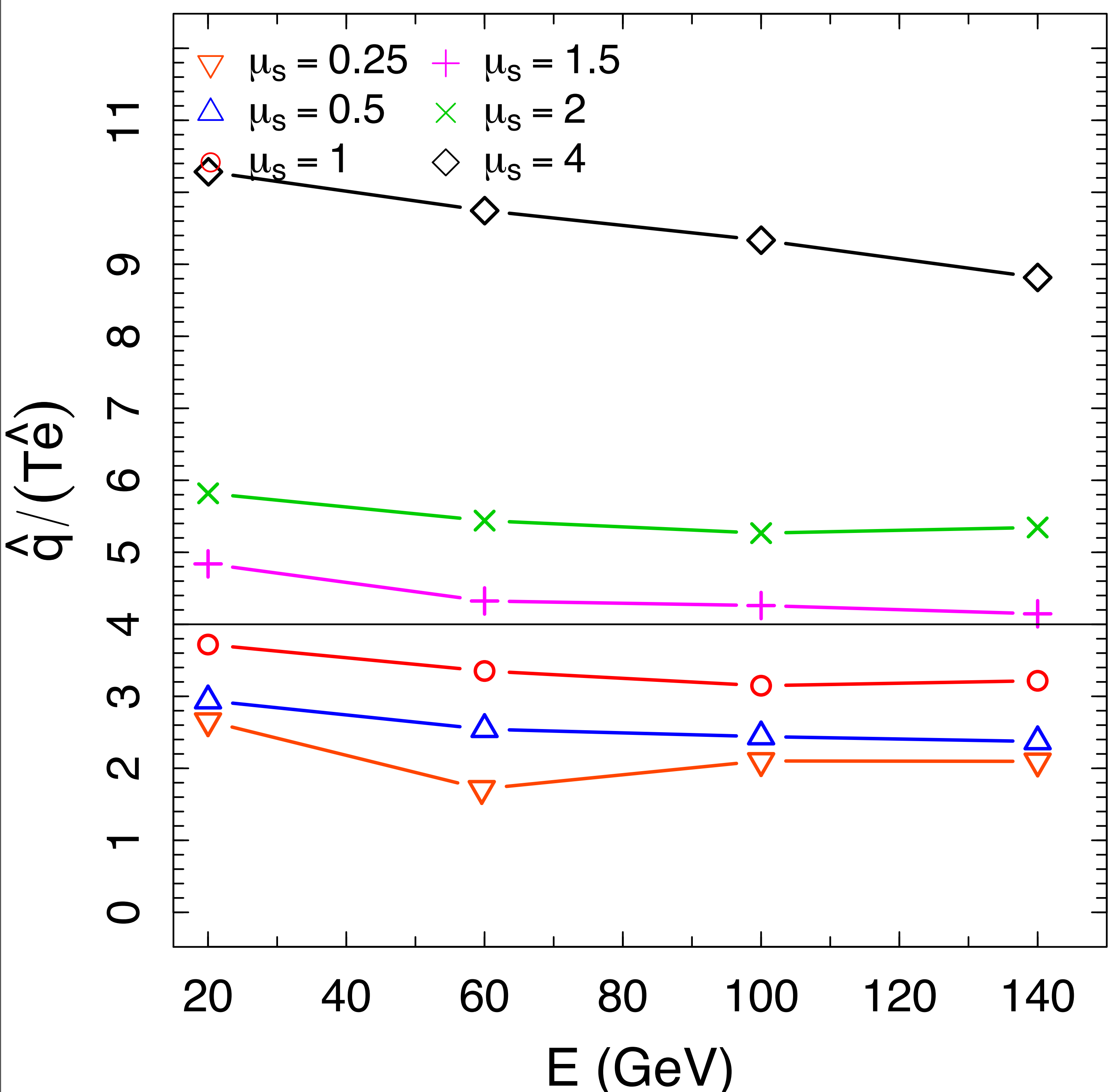

- Ratio scales linearly with the medium mass scale μs.
- Experimental measurements of q-hat and e-hat could provide insight into the nature of the QGP as seen by jets.
- Measurements made at different jet scales may reveal structure in quasi-particle mass spectrum.
- A possible precision measurement of hard probes and the QGP

Dijet Response at RHIC - Aj

T=350 MeV, Et > 20GeV

Varying mu-s

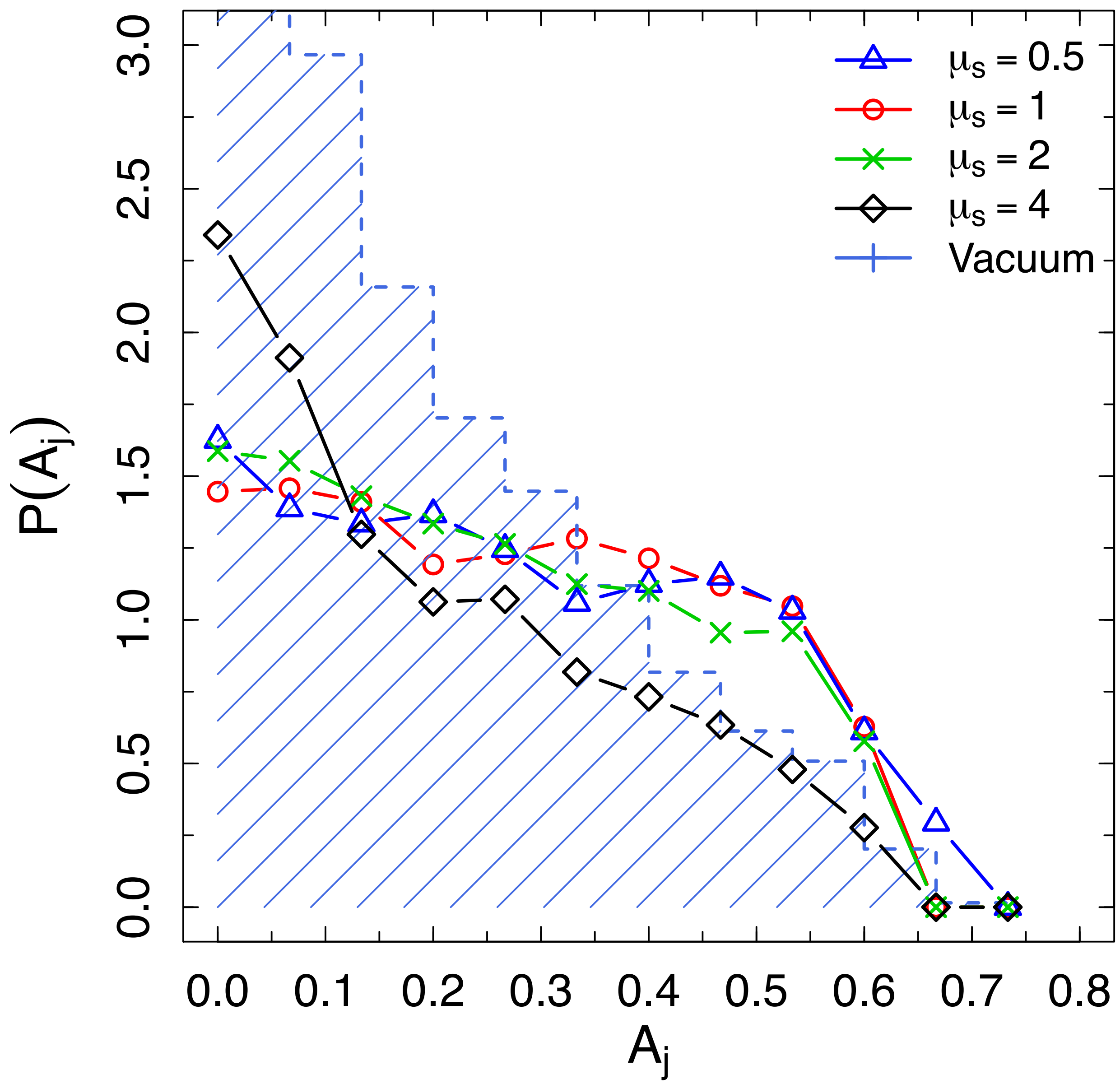

Varying alpha-s

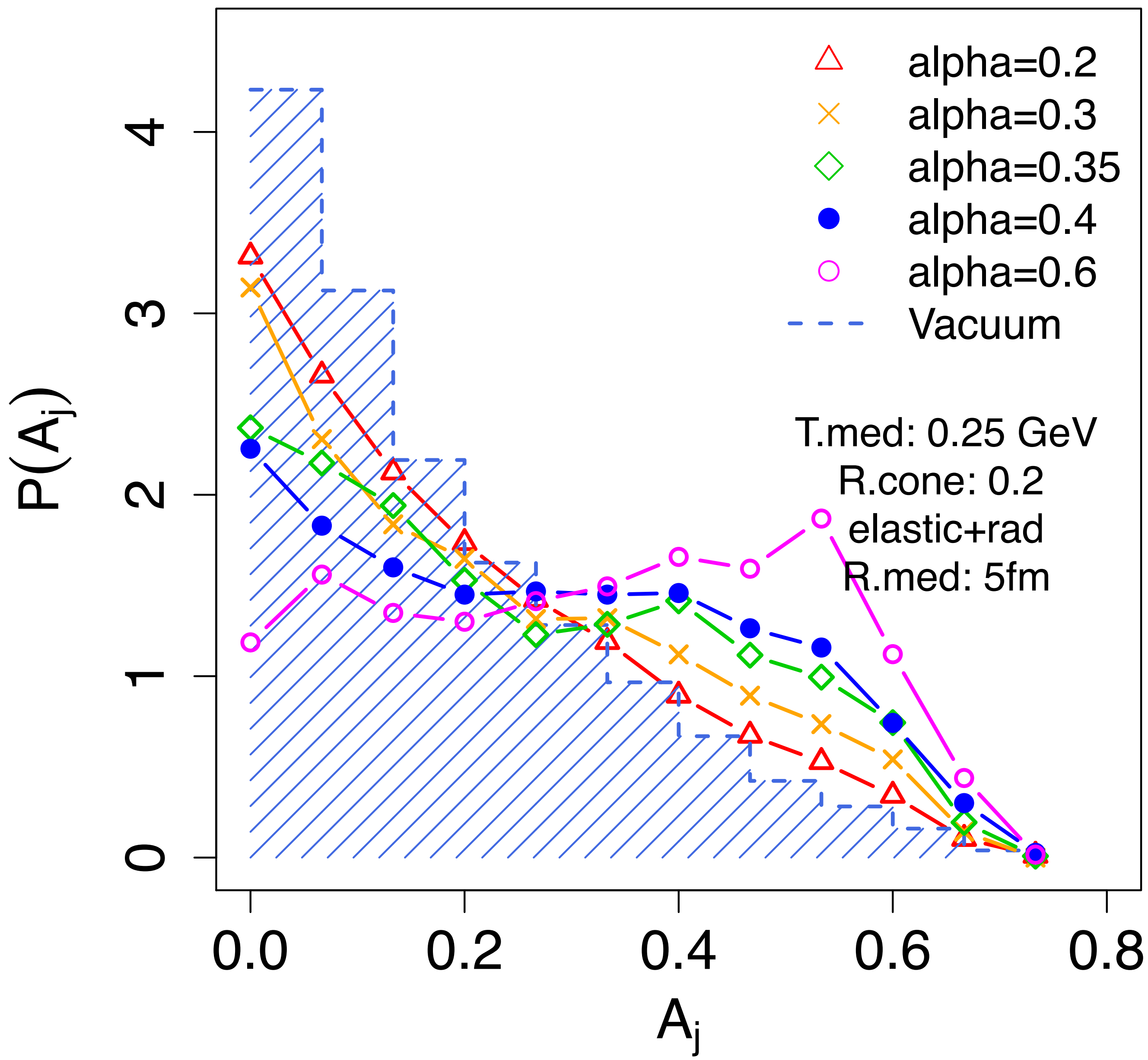

Elastic Interactions Only

Dijet Response at RHIC - Subleading Jet Shape

Varying mu-s

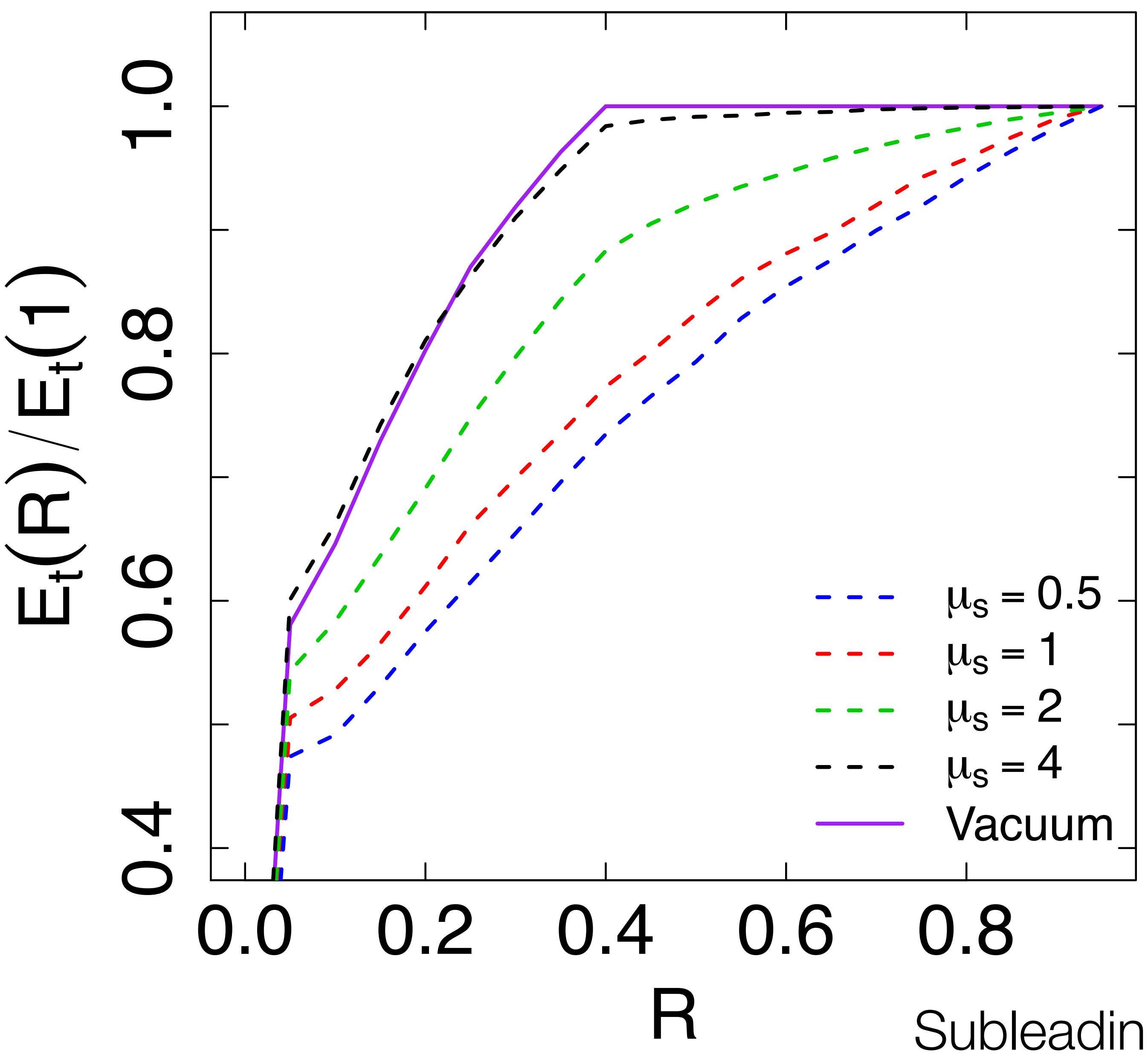

Varying alpha-s

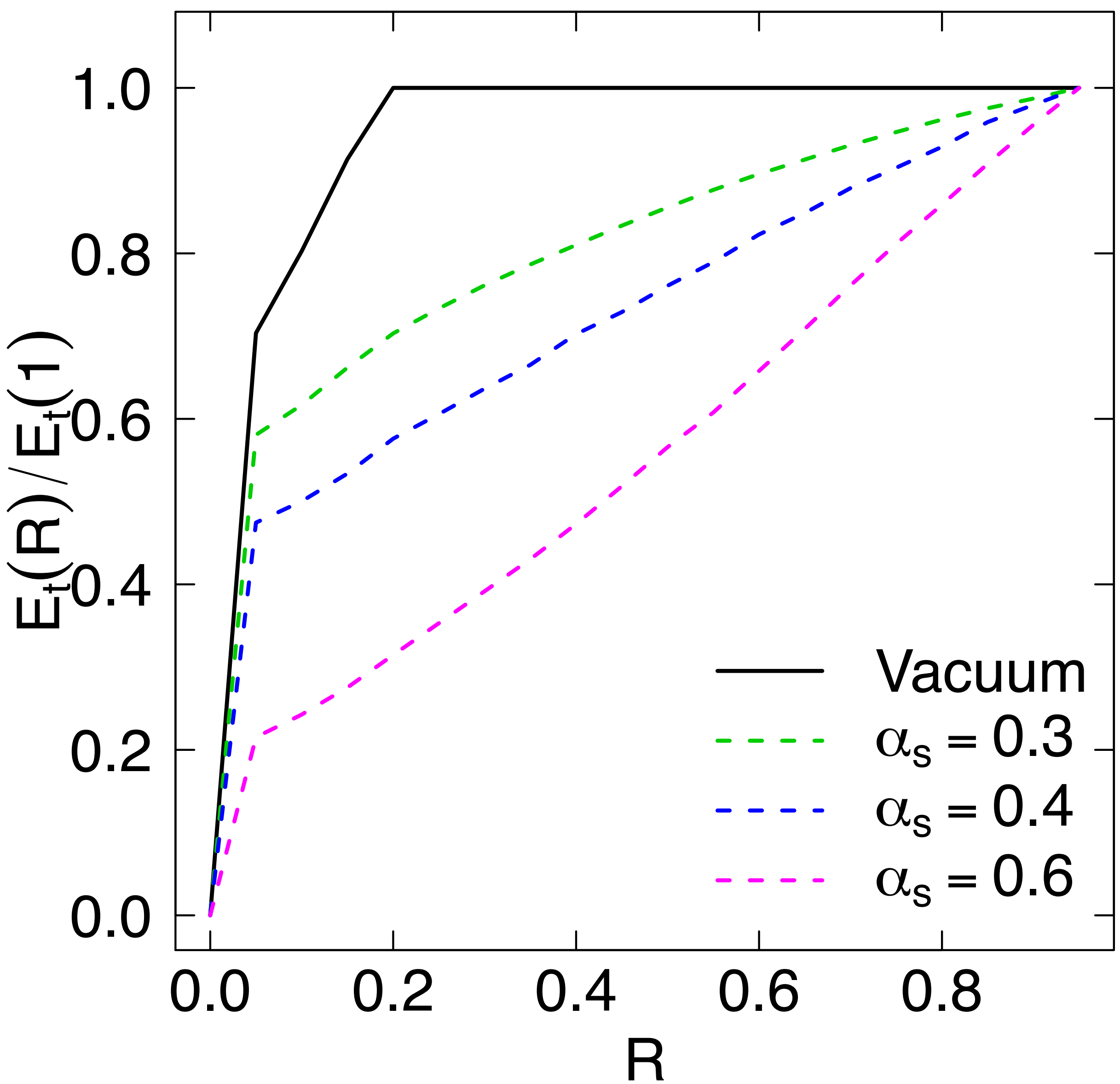

Subleading Jet Shape

Jet shape is sensitive to elastic energy loss

RHIC: Other Sensitive Observables?

$$J_T = E_T \sin \Delta R$$

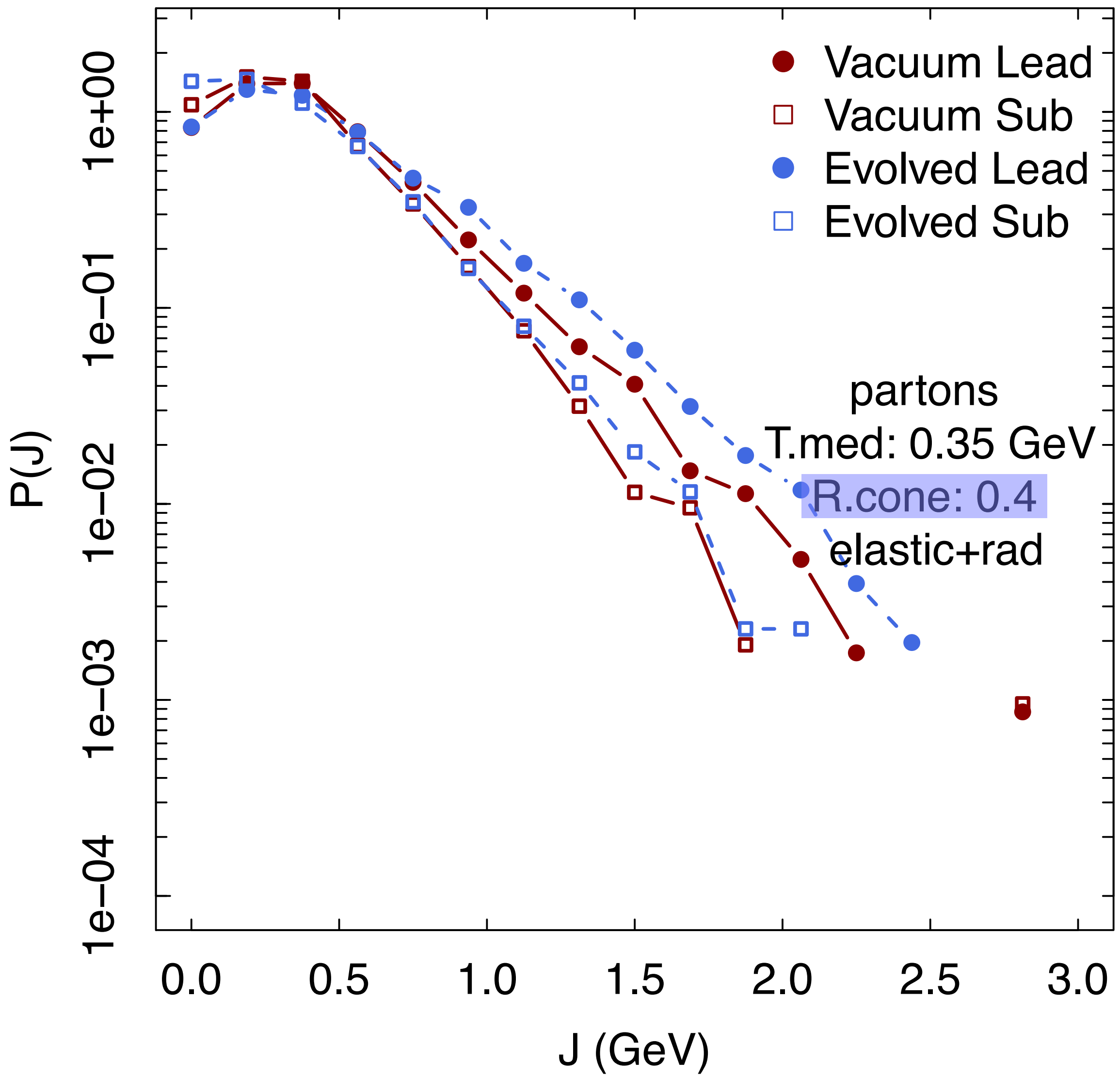

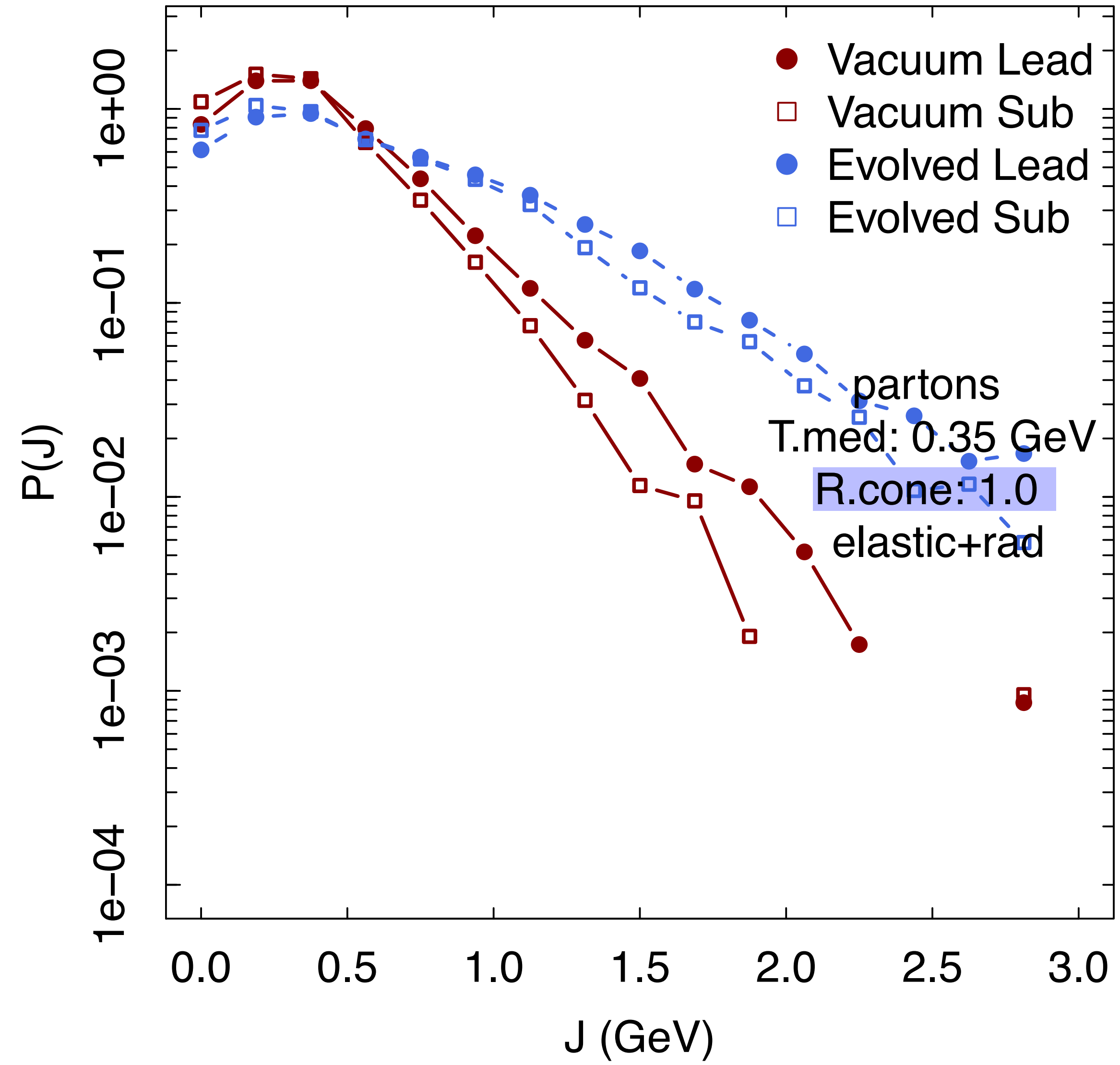

Narrow jets fragment similarly to vacuum

Extract Q-Hat from transverse fragmentation broadening?

R=1.0 jets show strong transverse broadening

VNI/BMS - 2.0 + Hydro

Keep jetty partons at each time step. Discard ‘old’ medium partons

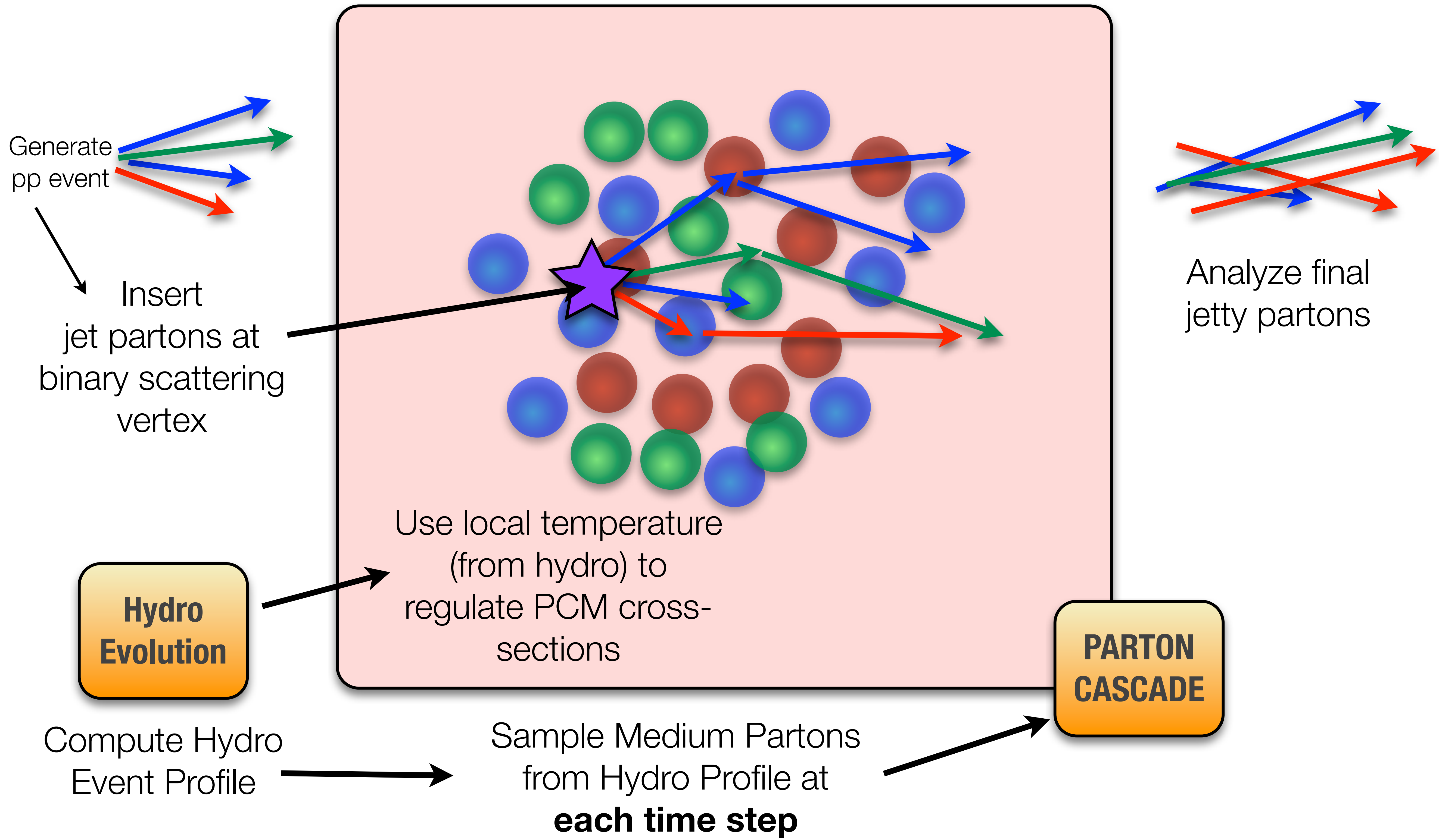

VNI/BMS - 2.0 Current + Future Features

- Elastic and Radiative energy loss models, with BDMPS-Z LPM effect
- Lund Stringy Hadronization with full color tracking from the initial generator.
- Fixed medium temperature in simple box mode.
- Event by event hydro background.
- Variable medium constituent masses give control of qhat/ehat ratio.
- Integration with Pythia for hard process generation
- Jet level data analysis built in (and single hard probe)
- Relatively simple user-options
- Modern build system (CMAKE)

Conclusions

- Is there a place for Parton Cascade Models in the future?
- Tracking full shower evolution seems to be key to understanding full jet observables. Do we need to use a full Parton Cascade to do this? Lattice Boltzmann
- Hydro is a very good description of the bulk dynamics. Can 'fake' this by ramping up cross-sections, at the cost of understanding the physics.
- Boltzmann equation allows treatment of non-equillibrium systems. Perhaps returning to the basic ideas would be interesting, PCM + CGC as an IC generator for hydro?

Extras

VNI/BMS Cross-Sections

g g → g g	$\frac{9}{2}\left(3-\frac{tu}{s^2}-\frac{su}{t^2}-\frac{st}{u^2}\right)$	q q′ → q q′	$\frac{4}{9}\frac{s^2+u^2}{t^2}$
q g→ q g	$-\frac{4}{9}\left(\frac{s}{u}+\frac{u}{s}\right)+\frac{s^2+u^2}{t^2}$	q qbar→ q′ qbar′	$\frac{4}{9}\frac{t^2+u^2}{s^2}$
g g → q qbar	$\frac{1}{6}\left(\frac{t}{u}+\frac{u}{t}\right)-\frac{3}{8}\frac{t^2+u^2}{s^2}$	q g →q γ	$-\frac{e_q^2}{3}\left(\frac{u}{s}+\frac{s}{u}\right)$
q q → q q	$\frac{4}{9}\left(\frac{s^2+u^2}{t^2}+\frac{s^2+t^2}{u^2}\right)-\frac{8}{27}\frac{s^2}{tu}$	q qbar → g γ	$\frac{8}{9}e_q^2\left(\frac{u}{t}+\frac{t}{u}\right)$
q qbar → q qbar	$\frac{4}{9}\left(\frac{s^2+u^2}{t^2}+\frac{u^2+t^2}{s^2}\right)-\frac{8}{27}\frac{u^2}{st}$	q qbar → γ γ	$\frac{2}{3}e_q^4\left(\frac{u}{t}+\frac{t}{u}\right)$
q qbar → g g	$\frac{32}{27}\left(\frac{t}{u}+\frac{u}{t}\right)-\frac{8}{3}\frac{t^2+u^2}{s^2}$		

- Dominant elastic interactions including screening mass

$$\mu_D = \sqrt{(2N_c + N_f)/6}gT$$

$$\frac{d\sigma^{gg\to gg}}{dq_\perp^2} = 2\pi\alpha_s^2\frac{9}{4}\frac{1}{(q_\perp^2+\mu_D^2)^2},$$

$$\frac{d\sigma^{gq\to gq}}{dq_\perp^2} = 2\pi\alpha_s^2\frac{1}{(q_\perp^2+\mu_D^2)^2},$$

$$\frac{d\sigma^{qq\to qq}}{dq_\perp^2} = 2\pi\alpha_s^2\frac{4}{9}\frac{1}{(q_\perp^2+\mu_D^2)^2},$$

Leading Parton Energy Loss

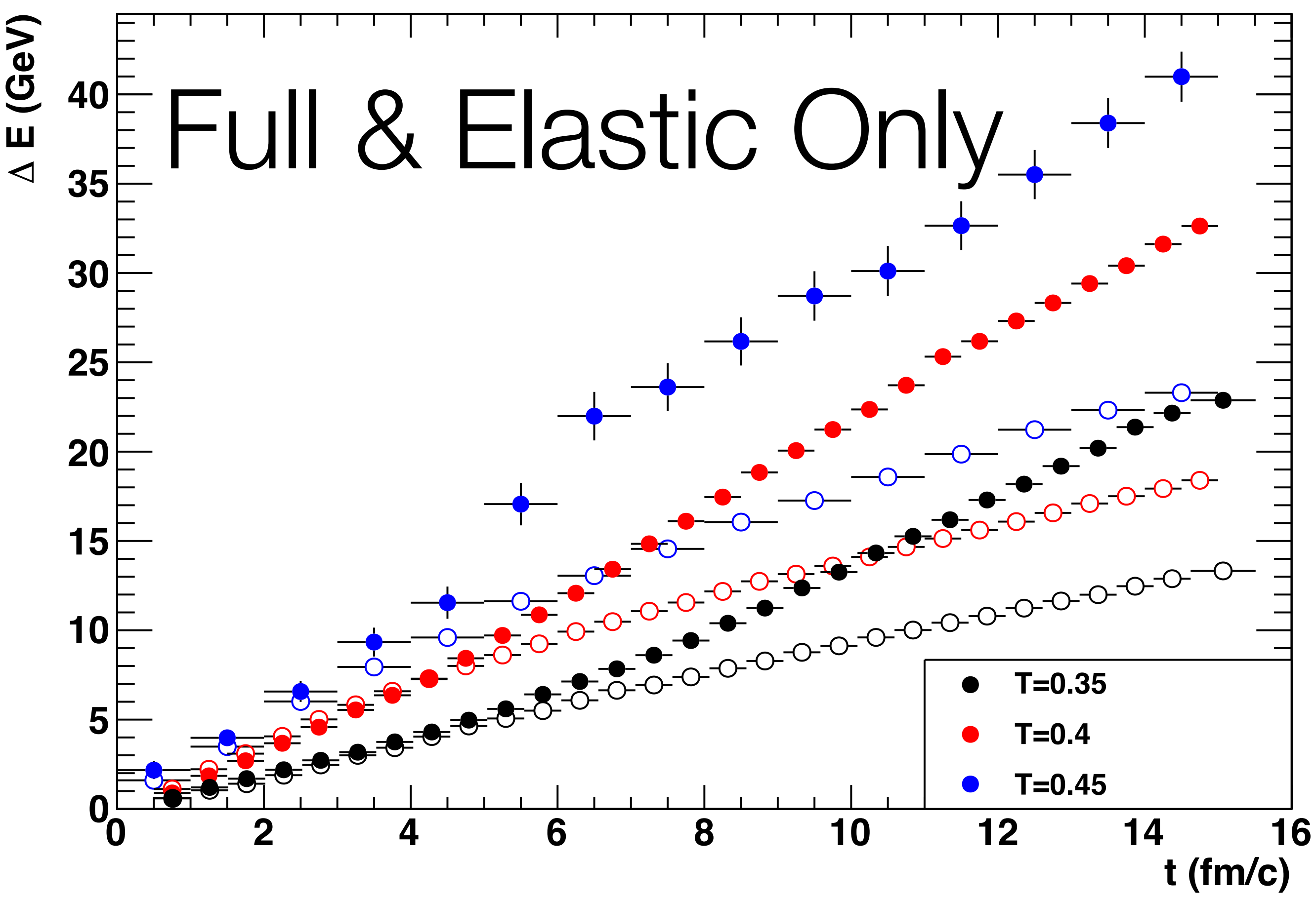

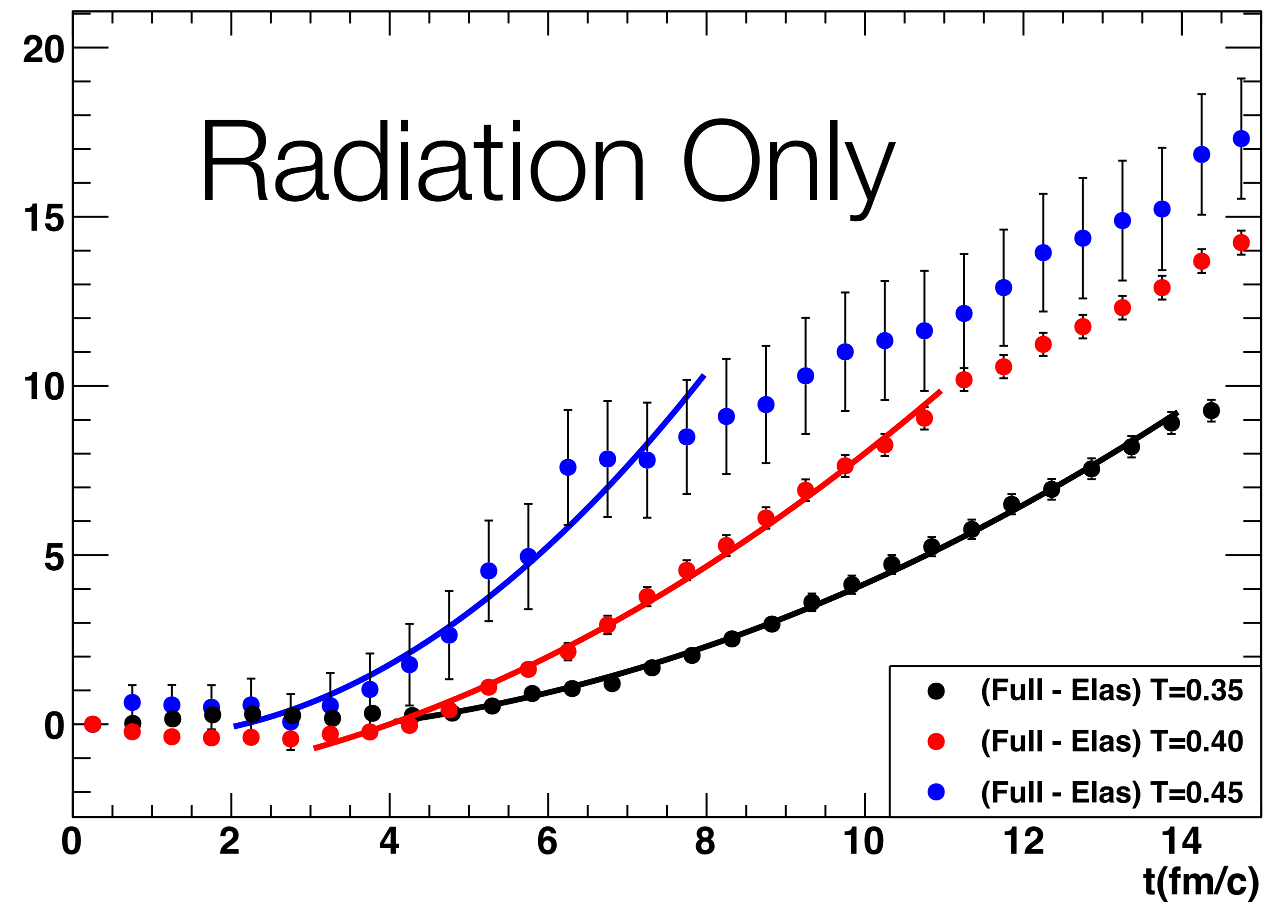

Radiation reproduces BDMPS-Z coefficient to 20%.

$$-\Delta E_{\mathrm{BDMPS}} = \frac{\alpha_s C_R}{8} \frac{\mu^2}{\lambda_g} L^2 \log \frac{L}{\lambda_g}.$$

Elastic (open circles) well described by pQCD results. $\Delta E_{elas} \propto T^2 L$

$$\hat{q} = \frac{1}{L} \sum_{i=1}^{N_{coll}} (\Delta p_{\perp,i})^2 = 2.2 \ (\mathrm{GeV}^2/\mathrm{fm})$$

T=0.35 GeV

Calibration of PCM elastic processes: Bass.S.A et al *J.Phys.G37105112* (2010)
Baier et al (BDMPS) *Nucl Phys.B478* (1996), B.Zakharov, *JETP Lett.63* (1996),